



# RESEARCH ACTIVITIES

## Photo-Molecular Science

We study the interaction between molecules and optical fields with its possible applications to active control of molecular functionality and reactivity. We also develop novel light sources to promote those studies. Two research facilities, the Laser Research Center for Molecular Science and the UVSOR, closely collaborate with the Department.

The core topics of the Department include ultrahigh-precision coherent control of gas- and condensed-phase molecules, high-resolution optical microscopy applied to nanomaterials, synchrotron-based spectroscopy of core-excited molecules and solid-state materials, vacuum-UV photochemistry, and the development of novel laser- and synchrotron-radiation sources.

# Development of Advanced Near-Field Spectroscopy and Application to Nanometric Systems

Department of Photo-Molecular Science  
Division of Photo-Molecular Science I



OKAMOTO, Hiromi  
NARUSHIMA, Tetsuya  
JIANG, Yuqiang  
HARADA, Yosuke  
LIM, Jong Kuk  
WU, Huijun  
NOMURA, Emiko

Professor  
Assistant Professor  
Post-Doctoral Fellow  
Post-Doctoral Fellow  
Post-Doctoral Fellow  
Graduate Student  
Secretary

There is much demand for the study of local optical properties of molecular assemblies and materials, to understand mesoscopic phenomena and/or to construct optoelectronic devices in the nanometric scale. Scanning near-field optical microscopy (SNOM) is an imaging method that enables spatial resolution beyond the diffraction limit of light. Combination of this technique with various advanced spectroscopic methods may offer a direct probe of dynamical processes in nano-materials. It may provide essential and basic knowledge for analyzing origins of characteristic features and functionalities of the nanometric systems. We have constructed apparatuses of near-field spectroscopy for excited-state studies of nano-materials, with the feasibilities of nonlinear and time-resolved measurements. They enable near-field measurements of two-photon induced emission and femtosecond transient transmission, in addition to conventional transmission, emission, and Raman-scattering. Based on these methods, we are investigating the characteristic spatiotemporal behaviors of various metal-nanoparticle systems and molecular assemblies.

## 1. Visualization of Plasmon Wavefunctions and Enhanced Optical Fields Induced in Metal Nanoparticles

We recently reported that wavefunctions of localized plasmon resonances of chemically synthesized metal (Au and Ag) nanoparticles are visualized by near-field transmission or two-photon excitation measurements.<sup>1,2)</sup> Figure 1(a) shows a typical near-field two-photon excitation image of the longitudinal plasmon mode on a Au nanorod, which correspond to the square modulus of the plasmon wavefunction. We also visualized optical fields in Au nanoparticle assemblies by the near-field two-photon excitation imaging method, as shown in Figure 1(b).<sup>1,3)</sup> It was revealed for the dimers that highly localized optical field is generated at the interstitial sites between the particles. In many-particle assemblies, the localized fields were especially intensified at the rim parts of the

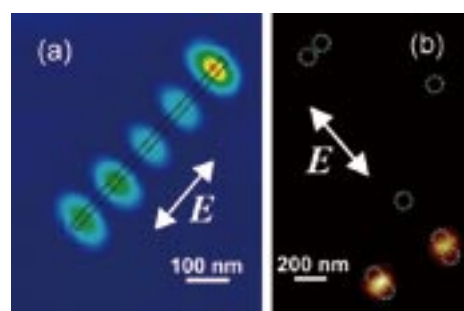


**Figure 1.** Near-field two-photon excitation images of (a) a Au nanorod (diameter 20 nm, length 540 nm), at 780 nm and (b) assembled Au spherical nanoparticles (diameter 100 nm).

assemblies.

We are now extending the studies to metal nanostructures manufactured by the electron-beam lithography technique, in collaboration with researchers of other institution, or other top-down fabrication techniques. Unique nano-optical characteristics, such as anomalous transmission enhancement through metal nanodisks, were found, and characteristic plasmon waves were observed for some metal nanostructures. Near-field properties of nano-void structures, opened on thin gold metallic films on glass substrates, have also been characterized, and the field distributions in the vicinities of the voids have been visualized. In circular void chain structures, we found that confined optical fields were generated in the interstitial sites between voids. The field distributions were analyzed based on the electromagnetic theories and calculations. Special attention has been paid for comparison of field distributions of complementary nanostructures, nanoparticle assembly and nano-void assembly, for instance, in relation to Babinet's principle in optics. Such a study is essential as a basis for designing unique optical properties and functions of metal nanostructures, and their applications to highly sensitive spectroscopic methods and exotic photochemical fields, as well as to nanoscale optical waveguides.

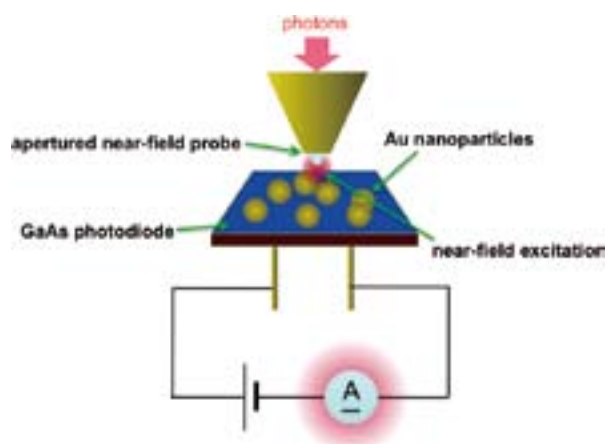


**Figure 2.** Schematic diagram of near-field photocurrent imaging measurement.

## 2. Studies of Metal-Nanostructure Modified Photovoltaic Cells by Near-Field Excited Site-Specific Photocurrent Detection

It has been known that metal nanoparticles and their assemblies collect photon energies to give confined and enhanced optical fields in the vicinities of the particles due to plasmon resonances, under suitably arranged conditions. Recently, it has been reported by a number of researchers that efficiencies of photoenergy conversion systems can be improved by the use of noble metal nanostructures. The photoenergy conversion system ranges from wet-type and solid-state photo-current conversion cells to photo-chemical conversion systems. To reveal the mechanism of the photoenergy conversion process and design more efficient conversion systems, studies of detailed nanostructures and site-dependence of photoirradiation effects are essential.

We applied SNOM to clarify effects of surface plasmon resonance on photo-current conversion in inorganic semiconductor photovoltaic cells modified with metal nanoparticles, where the photocurrent is reported to be enhanced compared with unmodified cells based on macroscopic measurements. The spatial characteristics of photocurrent for GaAs photodiodes with gold nanoparticles (nanospheres and nanorods) dispersed on the active surfaces were investigated by photocurrent imaging using a SNOM (Figure 2). In the case of gold nanospheres (diameter 100 nm), near-infrared light irradiation (785 nm) gave rise to the enhancement of photocurrent, resulted from re-radiation of photons *via* plasmon resonance on the gold nanosphere into the photovoltaic area, while photons in shorter wavelengths did not show enhanced photocurrent. In the case of gold nanorod, characteristic spatial oscillation of photocurrent caused by the longitudinal plasmon mode of the rod was observed. We are now analyzing the results obtained based on the near-field optical characteristics of the metal nanoparticles.

### Award

HARADA, Yosuke; Nano Optics Award, 19<sup>th</sup> Research Symposium of Nano Optics Group, Optical Society of Japan.

## 3. Construction of Apparatuses for Nonlinear and Ultrafast Near-Field Spectroscopy

In previous studies we achieved ultrafast near-field imaging with a time resolution of  $\sim 100$  fs.<sup>2,4)</sup> To further extend the dynamical studies of plasmons, we are now developing basic technologies to achieve near-field time-resolved measurements with  $< 20$  fs time resolution. We are also constructing an apparatus for near-field/far-field microscopic nonlinear optical measurements based on the technique of atomic-force microscope.

## 4. Near-Field Imaging of Organic Molecular Assemblies and Hybrid Systems

We are studying nanometric structures and optical properties of organic molecular assemblies such as carbon nanotubes embedded in sugar polymer chains, LB films of functional conjugated molecules, and hybrid systems consist of metal nanoparticles and organic functional materials, mainly as collaborations with other research groups.

## 5. Nonlinear Effects in Optical Trapping

The optical trapping technique has been widely used in various areas to manipulate particles, cells, and so forth. The principle of trapping is based on the interaction between optical electric fields and induced linear polarizations. In the course of the studies on behavior of gold nanoparticles under pulsed laser fields, we have found a novel phenomenon of optical trapping of spherical gold nanoparticles arising from nonlinear polarization when we trap the nanoparticles by ultrashort near-infrared laser pulses. That is, the stable trap site (usually appears in the center of the focused beam) is split into two equivalent positions, and the split trap positions are aligned along the direction of the incident laser polarization. The split distance depends on the trapping-laser power and wavelength. We have found that the results were successfully interpreted in terms of the nonlinear polarization caused by the femtosecond pulses.

### References

- 1) H. Okamoto and K. Imura, *Prog. Surf. Sci.* **84**, 199–229 (2009).
- 2) K. Imura, T. Nagahara and H. Okamoto, *J. Phys. Chem. B* **108**, 16344–16347 (2004).
- 3) K. Imura, H. Okamoto, M. K. Hossain and M. Kitajima, *Nano Lett.* **6**, 2173–2176 (2006).
- 4) K. Imura and H. Okamoto, *Phys. Rev. B* **77**, 041401(R) (4 pages) (2008).

# Quantum-State Manipulation of Molecular Motions

Department of Photo-Molecular Science  
Division of Photo-Molecular Science I



OHSIMA, Yasuhiro  
HASEGAWA, Hirokazu  
BAEK, Dae Yul  
HAYASHI, Masato  
KITANO, Kenta  
MIYAKE, Shinichiro  
INAGAKI, Itsuko

Professor  
Assistant Professor\*  
IMS Fellow†  
Post-Doctoral Fellow  
Graduate Student‡  
Graduate Student  
Secretary

Molecules in gas phase undergo translational, rotational and vibrational motions in a random manner, and the total molecular system is a statistical ensemble that contains a number of molecules in many different states of motions. This research group aims to establish methods to manipulate the quantum-state distribution pertinent to molecular motions, by utilizing the coherent interaction with laser lights. Here lasers with ultimate resolution in time and energy domains are employed complementally and cooperatively for manipulation of molecular motions.

## 1. Nonadiabatic Rotational Excitation of Molecules by Nonresonant Intense Femtosecond Laser Fields

When gaseous molecules are irradiated by an intense nonresonant ultrafast laser pulse, rotation of molecules is coherently excited via the interaction with the molecular anisotropic polarizability, to create a rotational quantum wave packet (WP). We have developed a method for exploring such a nonadiabatic rotational excitation (NAREX) process in a quantum-state resolved manner, and reported rotational-state distributions after the impulsive excitation with a fundamental output of a femtosecond (fs) Ti:Sapphire laser.<sup>1,2)</sup> Such a state-resolved investigation has afforded details concerning the excitation process during exposure to laser fields, and in a favorable case, full characterization of a rotational WP itself.<sup>3)</sup> In addition, frequency-domain studies can directly assess ultrafast control of the rotational-state distribution via the WP manipulation.<sup>4)</sup>

## 2. Ultrafast Angular-Momentum Orientation by Linearly Polarized Laser Fields<sup>5)</sup>

The anisotropy of molecular system is represented as a non-uniform distribution of projections,  $M$ , of angular momentum onto a space-fixed ( $Z$ ) axis. In particular, the system is designated as being *oriented* when the populations for  $+M$  and

$-M$  are different. In previous studies for the realization of orientation, circularly polarized radiation had been exclusively adopted, because it is regarded as the only way to induce the required helical interaction that breaks the right/left-handed symmetry around the  $Z$  axis. Recently, we show that a pair of linearly-polarized intense ultrafast pulses creates molecular ensembles with oriented rotational angular momentum in ultrafast time scale, when the delay and the mutual polarization between the pulses are appropriately arranged. The experimental result that demonstrates such an angular momentum orientation is shown in Figure 1.

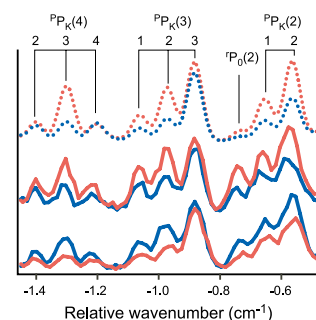


**Figure 1.** Excitation spectra of the  $S_1 \leftarrow S_0 6_0^1$  band of  $C_6H_6$  after fs double-pulse excitation. Blue and red lines correspond to right- and left-handed polarized probe pulses, respectively. The middle and lower panels are experimental ones for the mutual polarization angle of  $-\pi/4$  and  $\pi/4$ , while the upper is simulated one for  $-\pi/4$ .

## 3. Coherent Correlation between Nonadiabatic Rotational Excitation and Angle-Dependent Ionization of NO in Intense Laser Fields<sup>6)</sup>

When the intensity of the nonresonant ultrafast pulse is increased, the irradiated molecules are ionized as well as being rotationally excited. The coherent correlation between NAREX and the strong-field ionization in NO has been studied in the state-resolved manner. When the molecule is partly ionized in intense laser fields, a hole in the rotational WP of the remain-

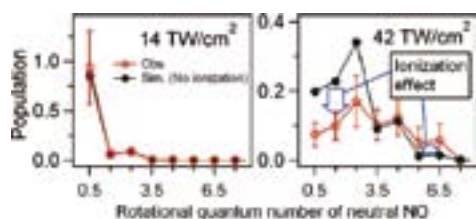


**Figure 2.** Rotational-state distribution of NO recorded after the excitation by a fs pulse at low (left) and high (right) intensity.

ing neutral NO is created by the ionization, whose rate depends on the alignment angle of the molecular axis with respect to the laser polarization direction. Rotational-state distributions of NO are observed and the characteristic feature that the population at higher  $J$  levels is increased by the ionization is identified, as shown in Figure 2. Numerical calculation for solving time-dependent Schrödinger equations including the effect of the ionization is carried out. The results suggest that the molecules aligned perpendicular to the laser polarization direction are dominantly ionized at the peak intensity of  $I_0 = 42 \text{ TW/cm}^2$ , where the multiphoton ionization is preferred rather than the tunneling ionization.

#### 4. Nonadiabatic Vibrational Excitation of Molecular Clusters by Nonresonant Intense Femtosecond Laser Fields

Nonadiabatic interactions with a nonresonant ultrafast laser field can coherently excite molecular vibration. The quantum-state resolved approach with ns probe pulses will also contribute to the study of nonadiabatic excitation of molecular vibration. The best candidates are van der Waals (vdW) clusters, since the librations of constituent molecules in

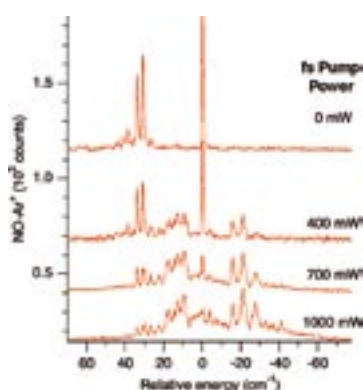


**Figure 3.** Excitation spectra of the A←X (0,0) band of NO–Ar after fs pulse excitation.

#### Award

KITANO, Kenta; Best Presentation Awards at the Annual Meeting of Japan Society for Molecular Science, 2009.

\* Present Address; The University of Tokyo, Graduate School of Arts and Sciences, Department of Basic Science, Tokyo 153-8902

† Present Address; University of Electro-Communications, Institute for Laser Science, Tokyo 182-8585

‡ Present Address; The University of Tokyo, Institute for Solid State Physics, Chiba 277-8581

vdW clusters have wide amplitudes and such intermolecular motions are inherently associated with large modulation of polarizability, yielding to strong Raman activities. We have indeed observed nonadiabatic vibrational excitation for the NO–Ar cluster. After the excitation with an intense fs pulse, several hot bands came to appear, as shown in Figure 3.

#### 5. High-Resolution Laser Spectroscopy of Benzene Clusters with He Atoms

Electronic spectra of benzene–(He)<sub>1,2</sub> clusters have been recorded via two-color resonant two-photon ionization with a single-mode ns-pulsed light source, consisting a dye amplifier injection-seeded by the CW output from a Ti:Sapphire laser. Owing to the narrow band width (~250 MHz) of the laser system and the efficient rotational cooling down to 0.3 K by implementing a high-pressure pulsed valve, rotational fine structures have been fully resolved in the observed spectra, as shown in Figure 4. Several vibronic bands associated to excitation of intermolecular vibrations have also been observed with rotational resolution. Their positions are reasonably matched with the prediction based on a high-level *ab initio* calculation.

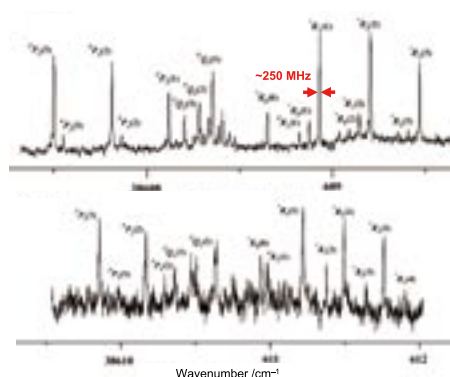


**Figure 4.** High-resolution excitation spectra of the  $S_1 \leftarrow S_0 6_0^1$  band of  $C_6H_6$ –He (top) and  $C_6H_6$ –(He)<sub>2</sub> (bottom).

#### References

- 1) H. Hasegawa and Y. Ohshima, *Phys. Rev. A* **74**, 061401 (2006).
- 2) H. Hasegawa and Y. Ohshima, *Chem. Phys. Lett.* **454**, 148 (2008).
- 3) H. Hasegawa and Y. Ohshima, *Phys. Rev. Lett.* **101**, 053002 (2008).
- 4) Y. Ohshima and H. Hasegawa, *Int. Rev. Phys. Chem.* **29**, 619 (2010).
- 5) K. Kitano, H. Hasegawa and Y. Ohshima, *Phys. Rev. Lett.* **103**, 223002 (2009).
- 6) R. Itakura, H. Hasegawa, Y. Kurosaki, A. Yokoyama and Y. Ohshima, *J. Phys. Chem. A* **114**, 11202 (2010).



# Development of High-Precision Coherent Control and Its Applications

Department of Photo-Molecular Science  
Division of Photo-Molecular Science II



OHMORI, Kenji  
KATSUKI, Hiroyuki  
TAKEI, Nobuyuki  
VESHAPIDZE, Giorgi  
IBRAHIM, Heide  
GOTO, Haruka  
NAKAGAWA, Yoshihiro  
INAGAKI, Itsuko

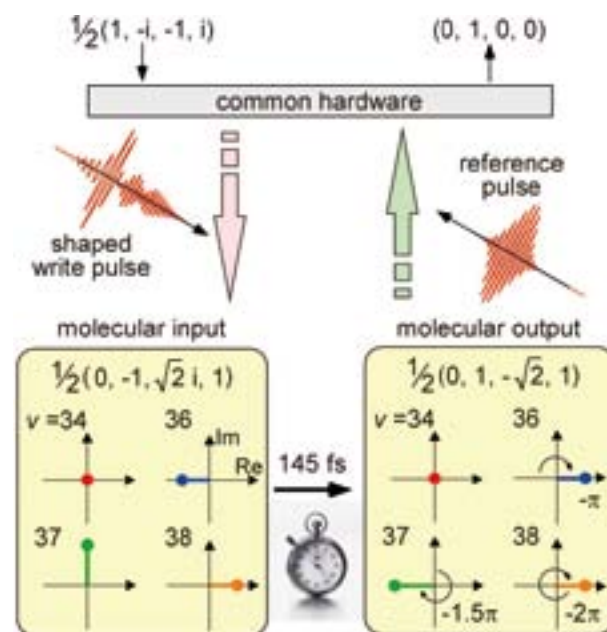
Professor  
Assistant Professor  
Assistant Professor  
Visiting Scientist; JSPS Post-Doctoral Fellow  
Visiting Scientist; JSPS Post-Doctoral Fellow  
Graduate Student  
Graduate Student  
Secretary

Coherent control is based on manipulation of quantum phases of wave functions. It is a basic scheme of controlling a variety of quantum systems from simple atoms to nanostructures with possible applications to novel quantum technologies such as bond-selective chemistry and quantum computation. Coherent control is thus currently one of the principal subjects of various fields of science and technology such as atomic and molecular physics, solid-state physics, quantum electronics, and information science and technology. One promising strategy to carry out coherent control is to use coherent light to modulate a matter wave with its optical phase. We have so far developed a high-precision wave-packet interferometry by stabilizing the relative quantum phase of the two molecular wave packets generated by a pair of femto-second laser pulses on the attosecond time scale. We will apply our high-precision quantum interferometry to gas, liquid, solid, and surface systems to explore and control various quantum phenomena.

## 1. Ultrafast Fourier Transform with a Femtosecond Laser Driven Molecule<sup>1)</sup>

Wave functions of electrically neutral systems can be used as information carriers to replace real charges in the present Si-based circuit, whose further integration will result in a possible disaster where current-leakage is unavoidable with insulators thinned to atomic levels. We have experimentally demonstrated a new logic gate based on the temporal evolution of a wave function. An optically tailored vibrational wave-

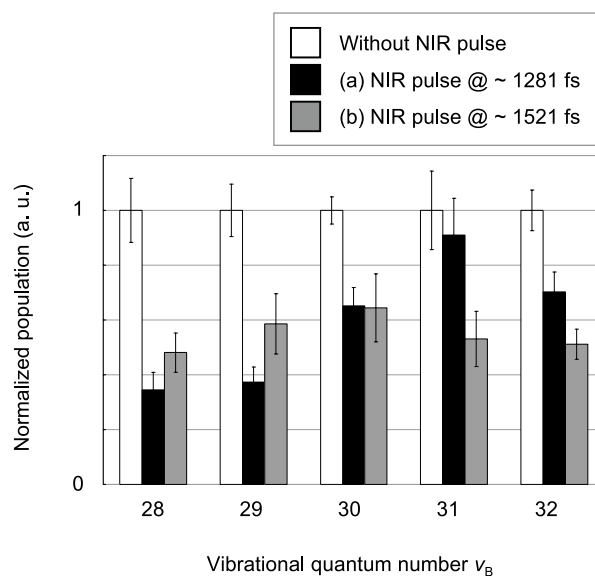
packet in the iodine molecule implements 4- and 8-element discrete Fourier-transform with arbitrary real and imaginary inputs. The evolution time is 145 fs, which is shorter than the typical clock period of the current fastest Si-based computers by three orders of magnitudes.



**Figure 1.** Schematic of the present discrete Fourier transform with an example:  $\frac{1}{2}(1, -i, -1, i) \rightarrow (0, 1, 0, 0)$ . The common transform matrices  $w_4$  and  $w_4^{-1}$  are operated for any arbitrary inputs and outputs, respectively, by the indicated hardware.




## 2. Optical Modification of the Vibrational Distribution of the Iodine Molecule<sup>2)</sup>

We have demonstrated previously that one can read and write information in a diatomic molecule as the population distribution which referred to as a “population code” [*Phys. Rev. Lett.* **104** (2010) 180501; *Phys. Rev. Lett.* **96** (2006) 093002; *Phys. Rev. A* **76** (2007) 013403]. As a next step to this read and write process, modification of the population code is necessary to develop logic gates. Here we demonstrate that the population code in the iodine molecule can be modified by near-infrared femtosecond laser pulses.



**Figure 2.** The vibrational distribution of the iodine molecule has been modified with a near-infrared femtosecond laser pulse.

### References

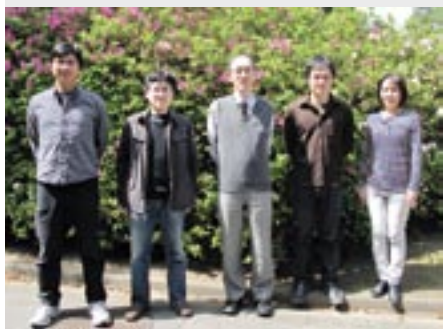
- 1) K. Hosaka, H. Shimada, H. Chiba, H. Katsuki, Y. Teranishi and K. Ohmori, *Phys. Rev. Lett.* **104**, 180501 (2010).  
 Selected for “Editors’ Suggestions” in PRL.  
 Covered by Physics **3**, 38 (2010).  
 Covered by Nature **465**, 138–139 (2010).
- 2) H. Goto, H. Katsuki and K. Ohmori, *Chem. Phys. Lett.* **493**, 170–172 (2010).

### Award

OHMORI, Kenji; Fellow of the American Physical Society.

# Molecular Inner-Shell Spectroscopy: Local Electronic Structure and Intermolecular Interaction

Department of Photo-Molecular Science  
Division of Photo-Molecular Science III



KOSUGI, Nobuhiro  
YAMANE, Hiroyuki  
NAGASAKA, Masanari  
NAKANE, Junko

Professor  
Assistant Professor  
Assistant Professor  
Secretary

In order to reveal local electronic structures and weak intermolecular interactions in molecular solids, liquids, and clusters, we are developing and improving several kinds of soft X-ray spectroscopic techniques such as XPS, XAS, RAS, XES, RXES, and RIXS at UVSOR in-vacuum undulator beamlines BL-3U and BL-6U with some international collaboration programs, and also an original *ab initio* quantum chemical program package GSCF, which is optimized to calculation of molecular inner-shell processes.

## 1. Inner-Shell Spectroscopy and Exchange Interaction of Rydberg Electrons Bound by Singly and Doubly Charged Kr and Xe Atoms in Small Clusters<sup>1)</sup>

Surface-site resolved Kr  $3d_{5/2}$  and Xe  $4d_{5/2}$  ionized states and Kr  $3d_{5/2}^{-1}5p$  and  $3d_{5/2}^{-1}6p$  and Xe  $4d_{5/2}^{-1}6p$  and  $4d_{5/2}^{-1}7p$  Rydberg excited states in small van der Waals Kr and Xe clusters with a mean size of  $\langle N \rangle = 15$  are investigated by X-ray photoelectron spectroscopy (XPS) and X-ray absorption spectroscopy (XAS). Furthermore, surface-site resolved Kr  $4s^{-2}5p$ ,  $4s^{-2}6p$ , and  $4s^{-1}4p^{-1}5p$  shakeup-like Rydberg states in small Kr clusters are investigated by resonant Auger electron spectroscopy (RAS). As shown in Figure 1, the exchange interaction (EX) of the Rydberg electron with the surrounding atoms and the induced polarization (iPL) of the surrounding atoms in the singly and doubly ionized atoms are deduced from the experimental spectra to analyze different surface site contributions in small clusters. The induced polarization and exchange repulsion energies are almost proportional to the number of the nearest neighbor atoms. The present analysis indicates that small Kr and Xe clusters with  $\langle N \rangle = 15$  have an average or mixture structure between the fcc-like cubic and icosahedron-like spherical structures.

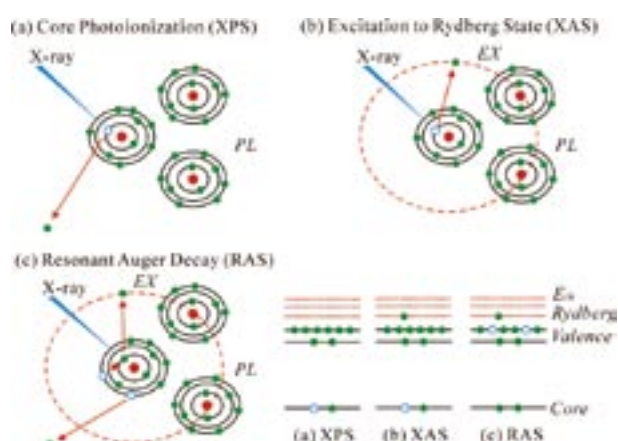


**Figure 1.** The final state in (a) XPS is stabilized by the induced polarization in clusters. The final states in (b) XAS and (c) spectator-like RAS are also stabilized by the induced polarization but are destabilized by the exchange interaction of the Rydberg electron with the surrounding atoms.

## 2. Vibrational Scattering Anisotropy Generated by Multichannel Quantum Interference in C1s- $\pi^*$ Resonance Auger Spectra of Acetylene<sup>2)</sup>

We measured the Fe 2p X-ray absorption spectra of decamethane. Based on angularly and vibrationally resolved electron spectroscopy measurements in acetylene, we report the first observation of anomalously strong vibrational anisotropy of RAS via the C1s- $\pi^*$  excited state with the strong Renner-Teller effect. We provide a model explaining this new phenomenon by three coexisting interference effects: (i) interference between resonant and direct photoionization channels, (ii) interference of the scattering channels through the core-



excited bending states with orthogonal orientation of the molecular orbitals, (iii) scattering through two wells of the double-well bending mode potential. The interplay of nuclear and electronic motions offers in this case a new type of nuclear wave packet interferometry sensitive to the anisotropy of nuclear dynamics: Whether which-path information is available or not depends on the final vibrational state serving for path selection.

### 3. Electric Field Effect on Electronic States in Organic Thin Films Studied by Fluorescence-Yield Soft X-Ray Absorption<sup>3)</sup>

In order to detect *in situ* electronic states of organic field effect transistor (OFET) in operation, we have utilized X-ray absorption spectroscopy (XAS) in the fluorescence yield (FY) mode. FY-XAS is a promising bulk-sensitive method for detection of inner electronic states of organic devices. To our best of knowledge, this is the first successful FY-XAS study on characterization of the organic devices under operating condition. Poly- and oligo-thiophenes are known to show high p-type-like performance. We fabricated 17nm-thick  $\alpha,\omega$ -dihexylsexithiophene (DH6T) films on the 500 nm-thick SiO<sub>2</sub> pre-covered Si substrates (highly B-doped, 0.5 mm-thick), and confirmed clear step-and-terrace morphology on the films by atomic force microscope. For the measurements of bias dependence, full-covered top-contact 25 nm-thick Au electrode was deposited on the DH6T thin films with cooling the substrate below 20 °C. The applied retarding bias exceeded -1 kV to shut out the photoelectrons excited by not only the fundamental X-rays but also the false second-order X-rays generated from gratings.

### 4. Site-Specific Intermolecular Interaction in $\alpha$ -Crystalline Films of Phthalocyanines Studied by Soft X-Ray Emission<sup>4)</sup>

The local electronic structures of crystalline and amorphous films of zinc phthalocyanine (ZnPc, C<sub>32</sub>H<sub>16</sub>N<sub>8</sub>Zn) and metal-free phthalocyanine (H<sub>2</sub>Pc, C<sub>32</sub>H<sub>18</sub>N<sub>8</sub>) have been studied using photon-in-photon-out type resonant X-ray emission spectroscopy (RXES) with a novel optical design based on a Wolter type I mirror, a transmission grating, and a back-illuminated charge couples device detector, which enables a high light-gathering capability without sacrificing the energy resolution. We found a clear crystalline structure dependence of the elastic-peak lineshape in RXES. As shown in Figure 2, the elastic peak observed for the crystalline films of ZnPc and H<sub>2</sub>Pc shows an asymmetric lineshape with resonant inelastic scattering (RIXS) structures, which cannot be observed for the amorphous films. The observed structure can be ascribed to the interplay of the intermolecular charge transfer excitation and the vibronic excitation that accompanies a direct recombination emission due to the Raman-active intermolecular interaction in crystalline phthalocyanine films.

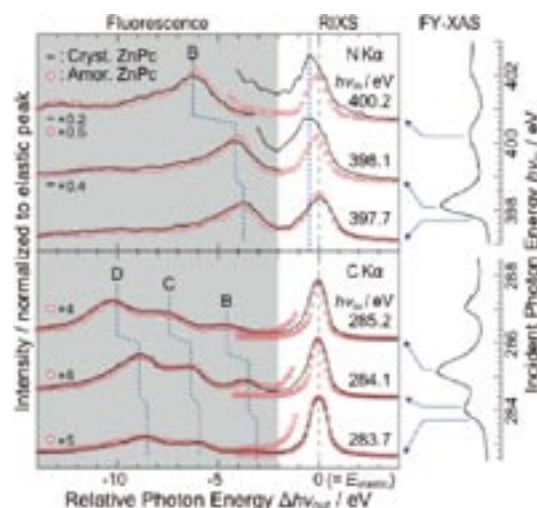


**Figure 2.** C and N K $\alpha$  RXES and RIXS spectra for the crystalline and amorphous ZnPc films. The abscissa is the energy difference between emitted and incident photons  $\Delta h\nu_{out}$  ( $= h\nu_{out} - h\nu_{in}$ ). All the spectra are normalized to the elastic peak intensity. The spectra for the crystalline and amorphous ZnPc films are shown using solid curves (black) and opened circles (red), respectively. The C and N K-edge FY-XAS spectra for the crystalline ZnPc film are shown in the right panel.

### 5. Orientation of *n*-Alkane in Thin Films on Graphite (0001) Studied by Soft X-Ray Absorption<sup>5)</sup>

We observed soft X-ray absorption spectra at the carbon K-edge of *n*-C<sub>12</sub>H<sub>26</sub> films grown on graphite (0001). The C1s-to- $\sigma^*_{CH}$ +Rydberg resonance directed along the CH bond was observed at 286.9 eV for the first layer of the *n*-C<sub>12</sub>H<sub>26</sub> film on graphite. This indicates that the CCC plane of the molecule is parallel to the surface (flat-on orientation). As the film thickness increases, the C1s-to- $\sigma^*_{CH}$ +Rydberg resonance directed perpendicular to the CH bond grows at 288.0 eV, suggesting an increase in the number of molecules with the CCC plane perpendicular to the surface in a multilayer film.

#### References

- 1) M. Nagasaka, T. Hatsui, H. Setoyama, E. Rühl and N. Kosugi, *J. Electron Spectrosc. Relat. Phenom.* (2010), in press.
- 2) C. Miron, V. Kimberg, P. Morin, C. Nicolas, N. Kosugi, S. Gavriluk and F. Gel'mukhanov, *Phys. Rev. Lett.* **105**, 093002 (2010).
- 3) H. S. Kato, H. Yamane, N. Kosugi and M. Kawai, to be published.
- 4) H. Yamane, T. Hatsui, K. Iketaki, T. Kaji, M. Hiramoto and N. Kosugi, to be published.
- 5) O. Endo, H. Ozaki, R. Sumii, K. Amemiya, M. Nakamura and N. Kosugi, to be published.

# Photoabsorption and Photoionization Studies of Fullerenes and Development of High-Efficiency Organic Solar Cells

Department of Photo-Molecular Science  
Division of Photo-Molecular Science III



MITSUKE, Koichiro	Associate Professor
KATAYANAGI, Hideki	Assistant Professor
PRODHAN, Md. Serajul Islam	Post-Doctoral Fellow
BASHYAL, Deepak	Graduate Student
ASARI, Chie	Technical Fellow
FUKUDA, Tatsuya	Technical Fellow

As the first topic, we have observed the formation of singly- and multiply-charged photoions from gaseous fullerenes irradiated with synchrotron radiation at  $h\nu = 25$  to 200 eV. We thus studied the mechanisms and kinetics of consecutive  $C_2$ -release reactions on the basis of (i) the yield curves for the fragments  $C_{60(70)-2n}^{z+}$  ( $n \geq 1$ ,  $z = 1-3$ ) as a function of the primary internal energy of the parent  $C_{60(70)}^{z+}$  and (ii) the three dimensional velocity distributions of the fragment carbon clusters.

In the second topic we have fabricated dye-sensitized solar cells (DSSC) containing ruthenium dye and iodide electrolyte and measured their short current and the intensity of the transmitted light to estimate the wavelength dependence of the incidence photon-to-current conversion efficiency (IPCE) and photoabsorbance (ABS) in the range of 300 to 1000 nm. In addition, we evaluated the quantum yield (APCE) of DSSCs for the electron injection from the excited orbital of Ru dye to the conduction band of  $TiO_2$  nano particles. Our final goal is to develop DSSCs with high performance and long lifetime by improving ABS and APCE mainly in the near infrared region.

## 1. Feasibility Study on the Mass-Selected Velocity Map Imaging of Polyatomic Molecules and Fullerenes<sup>1)</sup>

A photoionization spectrometer for velocity map imaging (VMI) has been developed for measuring the scattering distribution of fragment ions from polyatomic molecules. The spectrometer contains a mass gate and an ion reflector which can discriminate ions with a particular mass-to-charge ratio  $m/z$ . The basic functions and feasibility of these devices were tested experimentally and theoretically. First, the photoions from Kr and  $C_{60}$  were extracted into a time-of-flight (TOF) mass spectrometer by pulsed or continuous electrostatic fields. When the pulse-application timing on the mass gate was tuned to a specific  $m/z$ , the peak of the selected ions alone was present on a TOF spectrum. Second, the performance of the

mass gate in the VMI spectrometer was investigated by the computer simulations of the ion trajectories of fragments from  $C_{60}$ . The initial three-dimensional velocity distribution of  $C_{58}^+$  was projected onto the image plane with an energy resolution better than 10 meV. The  $C_{58}^+$  image was free from the contamination of other ions, e.g.  $C_{60}^+$  and  $C_{56}^+$ .

## 2. Mass-Analyzed Velocity Map Imaging of Thermal Photofragments from $C_{60}$ <sup>2)</sup>

The velocity distributions of the fragments produced by dissociative photoionization of  $C_{60}$  have been measured in the extreme UV region for the first time (see Figure 1), by using a flight-time resolved velocity map imaging technique combined with a high-temperature molecular beam and synchrotron radiation. Values of the average kinetic energy release were estimated at 6 different photon energies with respect to five reaction steps of sequential  $C_2$  ejection, starting from  $C_{60}^{2+} \rightarrow C_{58}^{2+} + C_2$  to  $C_{52}^{2+} \rightarrow C_{50}^{2+} + C_2$ . The translational temperatures of the fragment ions were found to be lower than those obtained by laser multiphoton absorption of  $C_{60}$ . The kinetic energies released in the first to fourth steps increase with increasing  $h\nu$  and reach 0.35–0.5 eV at  $h\nu = 102$  eV, reflecting statistical redistribution of the excess energy in the transition state, whereas that in the fifth step leading to  $C_{50}^{2+}$  was exceptionally small.

## 3. Mass-Analyzed Velocity Map Imaging of Thermal Photofragments from $C_{70}$

When  $C_{70}$  fullerenes absorb extreme UV photons of synchrotron radiation, primary parent ions undergo stepwise  $C_2$  ejection to produce fragment ions containing even-numbered carbon atoms. We have measured (1) the yield curves of the  $C_{70-2n}^{2+}$  fragments ( $1 \leq n \leq 6$ ) from  $C_{70}$  by TOF mass spectrometry and (2) their translational temperatures by velocity

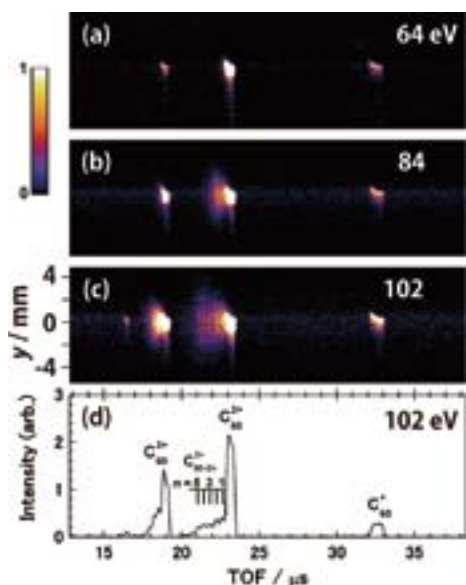


**Figure 1.** (a-c)  $y$ - $t$  maps of the photoions from  $C_{60}$  on which their counts are represented as a function of their arrival time  $t$  and the  $y$  coordinate of their incidence position on the PSD. The list-mode data at three  $h\nu$  positions are integrated over the whole  $x$  range. The  $y$  coordinate is proportional to the  $y$  component of the ion velocity. (d) TOF spectra of the photoions at  $h\nu = 102$  eV obtained by integrating the signal counts of (c) over the whole  $y$  range.

map imaging technique. The yield curve and translational temperature showed marked anomalies at  $n = 5$ , which may arise from exceptional stability of the  $C_{60}^{2+}$  fragments that have an icosahedral structure similarly to isolated  $C_{60}$  fullerene.

#### 4. Preparation and Evaluation of High Efficiency DSSCs<sup>3)</sup>

The high efficiency DSSCs were fabricated by using a screen-printing technique and a wet process. A  $TiO_2$  anode was immersed for 3 days in the acetonitrile solution of Ru complex compound (N719). The mixture of  $I_2$ , iodide salt, acetonitrile, etc. was used as a redox electrolyte. The counter electrode was covered with thin platinum film. The  $I$ - $V$  characteristics of DSSCs were recorded under simulated sun light (power density =  $100 \text{ mW cm}^{-2}$ ). The highest overall energy conversion efficiency was *ca.*  $\sim 8\%$ . The IPCE was calculated from the short current density and radiation power density as a function of the wavelength. The IPCE curve showed a peak of 0.73 at 535 nm. The performance and long-term stability of the DSSCs were studied by changing the thickness of the  $TiO_2$  film, the deposition method of the Pt film, and the compositions of the redox electrolyte.

#### 5. Azo Dyes as Photosensitizers for Organic Solar Cells<sup>4)</sup>

Fabrication and performance tests are reported on DSSCs containing azo dyes as photosensitizers. Fundamental properties of the DSSCs were obtained on the energy conversion

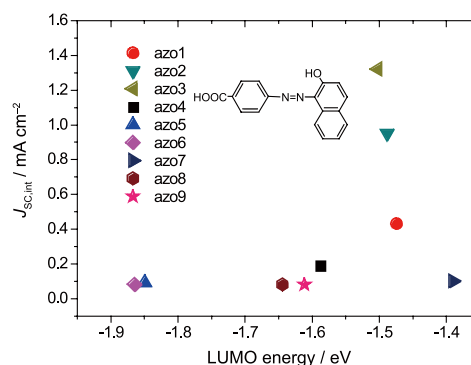


**Figure 2.** Correlation between the experimental data of the short current density of DSSCs and the theoretical energy levels of the LUMO of the solitary azo dyes.

efficiency  $\eta$ , short current and photoabsorbance in the wavelength range of 300 to 800 nm. Various azo dyes were synthesized in such a way that the positions and numbers of carboxylate and hydroxy groups differ from one dye to another. The carboxylate groups are considered to form strong linkages with the surface of  $TiO_2$  nanoparticles to promote rapid electron injection from dye molecules to the conduction band of  $TiO_2$ . We could demonstrate a remarkable correlation between the performance of the DSSCs and the energy level of the lowest unoccupied molecular orbital (LUMO) of the azo dye: no dye whose LUMO energy is lower than  $-1.5\text{eV}$  could allow us to make DSSCs with  $\eta > 0.1\%$  (see Figure 2). This finding is consistent with the necessary condition for the DSSC that the LUMO level should be higher than the lower bound of the conduction band of  $TiO_2$ .

#### 6. Transient Fluorescence Spectroscopy of DSSCs Using Picosecond Laser

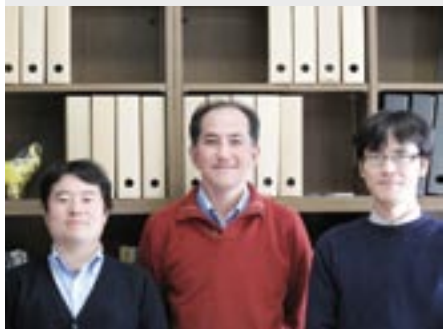
Observation was made on luminescence decay by time-resolved single photon counting using a picosecond laser  $\sim 470$  nm or free electron laser of  $\sim 580$  nm which operates at a repetition rate of 45 or 11.3 MHz, respectively. The apparent luminescence lifetime of the DSSC exposed to the air is longer than that preserved in vacuum, due to unwanted aggregation of the dye molecules at the surface of  $TiO_2$  of the former DSSC. The kinetics of electron injection will be discussed on the basis of the luminescence lifetime of various DSSCs and photo-voltaic electrodes

#### References

- 1) H. Katayanagi, B. P. Kafle, C. Huang, Md. S. I. Prodhon, H. Yagi and K. Mitsuke, *Proc. Pure and Applied Chemistry International Conference PACCON2010*, 941 (2010).
- 2) H. Katayanagi and K. Mitsuke, *J. Chem. Phys.* **133**, 081101 (2010).
- 3) Y. Poo-arporn, V. Vailikhit, D. Bashyal, K. Nakajima, P. Songsiririthikul and K. Mitsuke, *Proc. Pure and Applied Chemistry International Conference PACCON2010*, 424 (2010).
- 4) K. Nakajima, K. Ohta, H. Katayanagi and K. Mitsuke, *Proc. Pure and Applied Chemistry International Conference PACCON2010*, 967 (2010).

# Dynamics of Atoms & Molecules in Intense Laser Fields

Department of Photo-Molecular Science  
Division of Photo-Molecular Science III



HISHIKAWA, Akiyoshi  
FUSHITANI, Mizuho  
TSENG, Chien-Ming  
MATSUDA, Akitaka  
NAKANE, Junko

Associate Professor  
Assistant Professor  
IMS Fellow  
Post-Doctoral Fellow  
Secretary

Intense laser fields, comparable in magnitude with the Coulomb field within atoms and molecules, can be generated by focussing high-energy and ultrashort laser pulses. When exposed to such a strongly perturbing field, molecules exhibit various exotic features that cannot be observed in weak laser fields. We are seeking a deeper understanding of the behavior of molecules in intense laser fields, to elucidate how molecules interact with light, as well as to apply the new features they exhibit to the real-time visualization of ultrafast chemical reactions and their control. In particular, we focus on the following research directions:

- (A) Understanding of atomic and molecular dynamics in intense laser fields and the control
- (B) Ultrafast reaction imaging by laser Coulomb explosion imaging
- (C) Generation and application of ultrashort soft-X-ray pulses by laser high-order harmonics.

## 1. Development of Novel Photoelectron–Photoelectron Coincidence Spectrometer

Molecules in intense laser fields show characteristic reaction processes, such as above-threshold dissociation (ATD), bond softening/hardening and deformation of the geometrical structures. Since these interesting phenomena are all associated with rearrangement of the electron distribution by the intense laser fields, photoelectrons should provide direct information on how these reactions are induced. Here we developed a novel electron–electron–ion coincidence spectrometer to detect a pair of photoelectrons emitted simultaneously from a single molecule to understand the electron correlation dynamics in intense laser fields.

The spectrometer is based on a magnetic bottle type photoelectron spectrometer (see Figure 1). A strong permanent magnet located close to the FEL focus point provides an inhomogeneous magnetic field, which serves as a magnetic mirror for photoelectrons. The reflected photoelectrons are hence guided by the weak magnetic field of a long solenoid

toward a microchannel plate (MCP) detector placed at the end of a 1.5 m flight pass. The high collection efficiency with a  $4\pi$ -sr detection angle and the long light pass enables us to detect pairs of electrons emitted from a single atom. In order to securely identify the counter part ion, a pulsed high voltage is applied to the permanent magnet and ion collection electrodes to guide the ions to the same MCP detector used for electrons. The spectrometer was applied to double ionization of  $\text{CS}_2$  in IR (1.030  $\mu\text{m}$ ) intense laser fields, to reveal the ejection of the two electrons mostly proceeds sequentially at a field intensity of  $2.8 \times 10^{13} \text{ W/cm}^2$ .

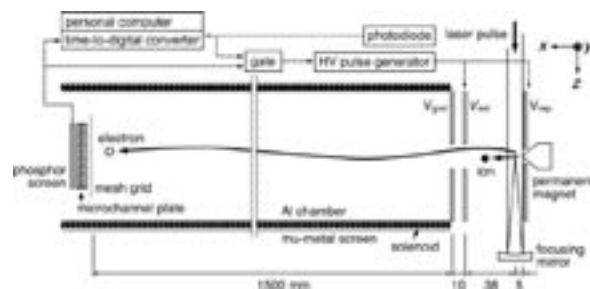


**Figure 1.** Schematic of photoelectron coincidence spectrometer equipped with collection electrodes for ion detection.

## 2. Visualization of Ultrafast Molecular Isomerization by Laser Coulomb Explosion Imaging

Novel features of molecules in intense laser fields can be utilized for new applications. Laser Coulomb explosion imaging is one such application, which provide a unique opportunity for real-time probing of large-scale structural changes in ultrafast chemical reactions.

Figure 2 shows the Newton diagram of three-body Coulomb explosion pathway of formaldehyde,  $\text{H}_2\text{CO}^{3+} \rightarrow \text{H}^+ + \text{H}^+ + \text{CO}^+$ . The diagram observed for the 7 fs case shows a clear and dense distribution of the  $\text{H}^+$  ion, located mostly in the first and fourth quadrant. The corresponding distribution for



the 35 fs case exhibits a significant broadening extending towards smaller momentum angle  $\theta_{\text{H-H}}$ . This finding shows that, when few-cycle intense laser pulses (7 fs) are used, the geometrical structure of the molecule is almost frozen along the H-C-H bending coordinate during the interaction with the laser pulse. On the other hand, significant deformation of the geometrical structure both along the C-H stretching and H-C-H bending coordinates is observed for the 35 fs laser pulses. The origin of the structural change can be understood in terms of the nuclear dynamics in the dication states populated in the rising edge of the laser pulse.

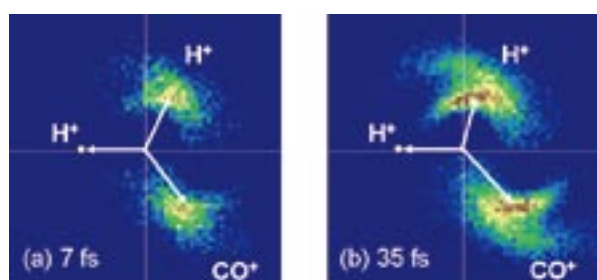


**Figure 2.** The Newton diagrams of  $\text{H}_2\text{CO}_3^+ \rightarrow \text{H}^+ + \text{H}^+ + \text{CO}^+$  in (a) 7 fs and (b) 35 fs intense laser fields, respectively. The amplitude of the linear momentum of the first  $\text{H}^+$  is normalized to unity and the normalized vector is placed on the negative  $x$ -axis.

### 3. Multiphoton Double Ionization of Ar in Intense Extreme Ultraviolet Laser Fields Studied by Shot-by-Shot Photoelectron Spectroscopy<sup>1)</sup>

Non-linear optical processes in extreme ultraviolet (EUV) and X-ray laser fields have attracted increasing attention after the advent of intense ultrashort free electron lasers (FEL), for their importance in a variety of applications, such as the creation of warm dense matter, optical switching and imaging of single bio-molecules. In addition to experiments on bulk materials, a number of experimental studies are devoted to clarify non-linear responses of isolated atoms, as they serve as an ideal benchmark for basic understanding on the non-linear EUV process in which both valence and core electrons can participate. We demonstrate that the shot-by-shot spectral monitoring of SASE FEL pulses and photoelectrons provides a clear understanding on the atomic responses to the intense EUV field. We have applied this technique to the multi-photon multiple ionization of Ar irradiated with SASE FEL pulses of mean photon energies around 21 eV. The sequential two-step double ionization due to three-photon absorption, (i)  $\text{Ar} + h\nu \rightarrow \text{Ar}^+ + e^-$  and (ii)  $\text{Ar}^+ + 2h\nu \rightarrow \text{Ar}^{2+} + e^-$ , is unambiguously identified as the dominant multiphoton pathway in a laser field of  $\sim 5 \text{ TW/cm}^2$ . Moreover, the shot-by-shot monitoring of the mean photon energies of the fluctuating FEL spectra clearly uncovered the effect of resonances in the sequential double ionization.

The  $\text{Ar}^{2+} 3p^{-2}$  structures shown in Figure 3 clearly show that both the peak intensities and profiles sensitively depend on the photon energy. This observation manifests the presence

of intermediate resonances in the two-photon ionization of  $\text{Ar}^{2+}$ . In fact, excited  $\text{Ar}^+$  states of the  $[3p^{-2}(^1D)]3d$  configuration lie close to the photoabsorption from  $\text{Ar}^+ 3p^{-1}$  as shown in Figure 3, and these  $\text{Ar}^{+*}$  states can generate resonances in the two-photon ionization of  $\text{Ar}^+$ . The intensity evolutions are dependent on the final  $\text{Ar}^{2+}$  levels, which implies that  $\text{Ar}^{+*}$  resonances are not common in the formations of these different  $\text{Ar}^{2+}$  levels.

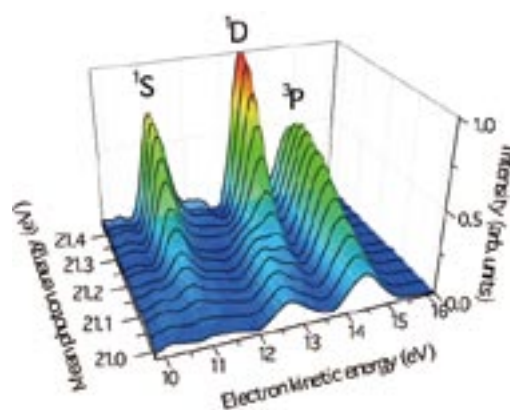


**Figure 3.** Photoelectron spectra in the range of the  $\text{Ar}^{2+} 3p^{-2}$  peaks, derived from a single-shot-basis analysis. In the analysis, the single-shot photoelectron spectra obtained at three different nominal FEL photon energies of 21.0, 21.2 and 21.4 eV were sorted by the mean photon energies determined from the  $\text{Ar}^+ 3p^{-1}$  peak energies, and then averaged within narrow photon energy ranges that divide the whole photon energy range into 13 segments.

### 4. Generation of Laser High-Order Harmonics and Application for Ultrafast Reaction Probing

Laser high-order harmonics have novel features such as i) photon energy higher than several 100 eV, ii) extremely short pulse duration in the sub-fs regime, iii) high-quality spatio-temporal coherence, iv) high photon flux comparable to synchrotron radiation and v) simple and precise synchronization with other laser light sources. Because of these aspects, the laser high-order harmonic pulses are of great interest as a potential light source for time-resolved spectroscopy of ultrafast dynamics that could not be elucidated in real time by conventional techniques. Preliminary pump-probe experiments on the photodissociation of  $\text{Br}_2$  show a steep rise ( $\sim 80$  fs) of the  $\text{Br}(^2P_{3/2})$  yields, reflecting a ultrashort pulse duration ( $< 20$  fs) of the 27th harmonic pulses used to probe the  $\text{Br}(^2P_{3/2})$  product. Full characterization of the temporal profile of the harmonic pulses and application to the time-resolved photoelectron imaging are in progress.

#### Reference

- 1) Y. Hikosaka, M. Fushitani, A. Matsuda, C.-M. Tseng, A. Hishikawa, E. Shigemasa, M. Nagasono, K. Tono, T. Togashi, H. Ohashi, H. Kimura, Y. Senba, M. Yabashi and T. Ishikawa, *Phys. Rev. Lett.* **105**, 133001 (2010).



# Light Source Developments by Using Relativistic Electron Beams

**UVSOR Facility**  
**Division of Advanced Accelerator Research**



KATO, Masahiro  
 ADACHI, Masahiro  
 ZEN, Heishun  
 TANIKAWA, Takanori  
 TAIRA, Yoshitaka  
 KIKUCHI, Yoshitaka

Professor  
 Assistant Professor  
 Assistant Professor  
 Graduate Student  
 Graduate Student\*  
 Graduate Student\*

This project involves researches and developments on synchrotron light source, free electron laser, beam physics and their related technologies. Most of these works are performed at the UVSOR-II electron storage ring and its injector.

## 1. Developments on UVSOR Accelerators

In these years, we have been preparing for a new injection method called top-up injection at UVSOR-II, which would remove the serious short beam lifetime problem caused by the small emittance and the low electron energy.<sup>1)</sup> In this operation scheme, electron beam is re-filled with a short interval, typically one minute, to keep the beam current almost constant.

In 2008, we have started test operation with the top-up injection on every Thursday night. Although the users experiments are greatly improved by the high and constant beam intensity, it was also found that, in some beam-lines, the instantaneous electron orbit movement during the injection affected the experimental data. We prepared a system to deliver beam injection timing signals to the beam-lines that enables the users to stop the data acquisition during the injection. We have also prepared a feedback system to stabilize the injection efficiency. In July 2010, we have started operating the machine with the top-up injection fully in the users beam time. A typical beam current history in a week is shown in Figure 1.

In spring 2010, we have reconstructed a part of the storage ring and the beam transport line to create a new 4 m straight section to install a new undulator which would be dedicated for light source developments. As shown in Figure 2, the beam transport line was extended, the injection pulse magnets, the RF cavity and some instruments for beam diagnostics were also moved. After the three month reconstruction work, the accelerator was successfully re-commissioned on schedule. An undulator system is under construction, which will be installed in the straight section in spring, 2011.

We are investigating some possibility of further upgrade of UVSOR-II as a future plan in near term. It was found that, by

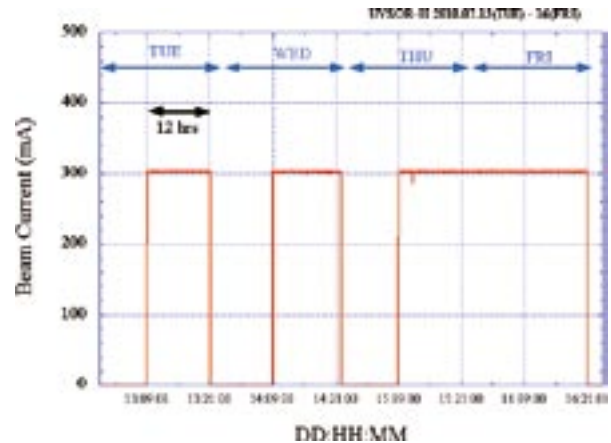


**Figure 1.** Beam current history in the top-up test operation in a week. The ring is operated for 12 hours on Tuesday and Wednesday, and 36 hours from Thursday to Friday in the top-up mode as keeping the beam current at 300mA.



**Figure 2.** A part of the storage ring and the beam transport line in spring 2010, before the reconstruction (left) and after (right). The beam transport line was extended and a new 4m straight section was created in the ring. The devices colored in blue are bending magnets.

introducing combined function bending magnets, the beam emittance could be reduced by a factor of 2. This upgrade would make UVSOR-II the world brightest low energy synchrotron light source. Other possibilities on the future plan are also under investigation, which include a ultra-low emittance storage ring, a linac-based free electron laser or an energy recovery linac.

## 2. Light Source Developments

A resonator-type free electron laser is operational at UVSOR. The wavelength is ranging from 800 nm to 199 nm and the average power exceeds 1W in visible and deep UV regions. In these years, it is used for users experiments<sup>2)</sup> and for basic researches on free electron laser physics. In the latter, coherent photon seeding was successfully demonstrated,<sup>3)</sup> in which a small fraction of the out-coupled laser light was re-injected to the optical cavity and the laser oscillation was drastically stabilized.

By utilizing the free electron laser optical cavity, we have developed a system to create micro-density structure on electron bunches circulating in the storage ring by using an external laser source.<sup>4)</sup> By controlling the laser pulse shape, we can create various density structures such as a short dip structure or a periodic structure. In the former case, broadband coherent terahertz radiation was produced<sup>4)</sup>. In the latter case, quasi-monochromatic coherent terahertz radiation was produced.<sup>5)</sup> Such a micro-density structure normally disappears very quickly after a few revolutions of the electron bunch in the storage ring, which is due to the synchrotron motion. Thus, the intense terahertz radiation also stops. To suppress this effect and maintain the terahertz radiation for a long period, we tried to operate the ring with a small momentum compaction factor. It was observed that the terahertz emission lasted for about ten revolutions. It was also observed that the THz intensity drastically changed revolution by revolution. This peculiar behavior could be explained by the coupling between the longitudinal motion and the transverse motion of the electrons.<sup>6)</sup>

Coherent harmonic generation is a method to produce coherent harmonics of laser light by using relativistic electron beam. The laser-electron interaction in an undulator produces density modulation of a period of the laser wavelength, which also contains harmonic components. Such an electron bunch radiates coherently at the harmonics of the injected laser. We have successfully observed the coherent harmonics of Ti:Sa laser in the VUV range, up to 9<sup>th</sup> harmonic.<sup>7)</sup>

The coherent radiation experiments using laser is supported by the Quantum Beam Technology Program of JST/MEXT. Under this support, a part of the storage ring was reconstructed as described above and a new undulator will be installed. The upgrade of the laser system was completed. Two new beam-lines dedicated to the coherent lights in the VUV range and in the THz range will be constructed.

Laser Compton scattering is a technique to produce a

quasi-monochromatic X-rays and gamma-rays by using a relativistic electron beam and laser. The laser photons are Compton back scattered by the high energy electrons and are converted to gamma-rays. We have successfully demonstrated that the energy of the gamma-rays could be changed continuously by changing the injection angle of the laser. It was expected that a femto-second gamma-ray pulses could be produced by injecting the laser from the vertical direction to the electron beam. The experiment is under going.

## 3. Developments of Accelerator Technologies

Beam diagnostic systems are important especially during the commissioning of a new storage ring or that just after a big reconstruction. In collaborating with Synchrotron Radiation Research Center in Nagoya University, we have developed a turn-by-turn beam position measurement system and a betatron tune measurement system. The former was to measure the beam position of the electron beam just after the injection. The electron orbit of each turn was successfully observed.<sup>8)</sup> In the latter, betatron tunes of the booster synchrotron during the acceleration was successfully measured. A suppression of the betatron motion due to the non-linear magnetic field was successfully observed.<sup>9)</sup>

### References

- 1) M. Katoh, M. Adachi, H. Zen, J. Yamazaki, K. Hayashi, A. Mochihashi, M. Shimada and M. Hosaka, presented at 10<sup>th</sup> Int. Conf. Synchrotron Rad. Instr. (Melbourne, 2009), to be published in *AIP Conf. Proc.*
- 2) J. Takahashi, H. Shinjima, M. Seyama, Y. Ueno, T. Kaneko, K. Kobayashi, H. Mita, M. Adachi, M. Hosaka and M. Katoh, *Int. J. Mol. Sci.* **10**, 3044–3064 (2009).
- 3) C. Evain, C. Szwaj, S. Bielawski, M. Hosaka, A. Mochihashi, M. Katoh and M.-E. Couprie, *Phys. Rev. Lett.* **102**, 134501 (2009).
- 4) M. Shimada, M. Katoh, S. Kimura, A. Mochihashi, M. Hosaka, Y. Takashima, T. Hara and T. Takahashi, *Jpn. J. Appl. Phys.* **46**, 7939–7944 (2007).
- 5) (in alphabetic order) S. Bielawski, C. Evain, T. Hara, M. Hosaka, M. Katoh, S. Kimura, A. Mochihashi, M. Shimada, C. Szwaj, T. Takahashi and Y. Takashima, *Nat. Phys.* **4**, 390–393 (2008).
- 6) M. Shimada, M. Katoh, M. Adachi, T. Tanikawa, S. Kimura, M. Hosaka, N. Yamamoto, Y. Takashima and T. Takahashi, *Phys. Rev. Lett.* **103**, 144802 (2009).
- 7) T. Tanikawa, M. Adachi, M. Katoh, J. Yamazaki, H. Zen, M. Hosaka, Y. Taira and N. Yamamoto, *Proc. 1<sup>st</sup> Int. Particle Acc. Conf.* 2206 (2010).
- 8) A. Nagatani, Y. Takashima, M. Hosaka, N. Yamamoto, K. Takami, M. Katoh, M. Adachi, H. Zen and K. Hayashi, *UVSOR Activity Report 2009* 34 (2010).
- 9) Y. Furui, M. Hosaka, N. Yamamoto, Y. Takashima, M. Adachi, H. Zen and M. Katoh, *UVSOR Activity Report 2009* 32 (2010).

\* carrying out graduate research on Cooperative Education Program of IMS with Nagoya University

# Synchrotron Radiation Spectroscopy on Strongly Correlated Electron Systems

UVSOR Facility  
Division of Advanced Solid State Physics



KIMURA, Shin-ichi	Associate Professor
MATSUNAMI, Masaharu	Assistant Professor
MIYAZAKI, Hidetoshi	IMS Fellow
MORI, Tatsuya	Post-Doctoral Fellow
NISHI, Tatsuhiko	Research Fellow*
MIZUNO, Takafumi	Graduate Student
IIZUKA, Takuya	Graduate Student
MITANI, Hiroyuki	Graduate Student†
HAJIRI, Tetsuya	Graduate Student‡

Solids with strong electron–electron interaction, so-called strongly correlated electron systems (SCES), have a various physical properties, such as non-BCS superconducting, colossal magneto-resistance, heavy fermion and so on, which cannot be predicted by first-principle band structure calculation. Due to the physical properties, the materials are the candidates of the next generation functional materials. We investigate the mechanism of the physical properties as well as the electronic structure of SCES, especially rare-earth compounds, organic superconductors and transition-metal compounds, by infrared/THz spectroscopy and angle-resolved photoemission spectroscopy based on synchrotron radiation. Since experimental techniques using synchrotron radiation are evolved rapidly, the development of the synchrotron radiation instruments is also one of our research subjects.

## 1. SAMRAI: A Variably Polarized Angle-Resolved Photoemission Beamline in the VUV Region at UVSOR-II<sup>1)</sup>

A novel variably polarized angle-resolved photoemission spectroscopy beamline in the vacuum-ultraviolet (VUV) region has been installed at the UVSOR-II 750 MeV synchrotron light source. The beamline is (shown in Figure 1) equipped with a 3 m-long APPLE-II type undulator with horizontally/vertically linear and right/left circular polarizations, a 10-m Wadsworth-type monochromator covering a photon energy range of 6–43 eV, and a 200 mm-radius hemispherical photoelectron analyzer with an electron lens of a  $\pm 18$ -degree acceptance angle. Due to the low emittance of the UVSOR-II storage ring, the light source is regarded as an entrance slit and the undulator light is directly led to a grating by two plane mirrors in the monochromator while maintaining a balance between high energy resolution and high photon flux. The energy resolving power ( $h\nu/\Delta h\nu$ ) and photon flux of the monochromator are typically  $1 \times 10^4$  and  $10^{12}$  photons/sec, respectively, with a

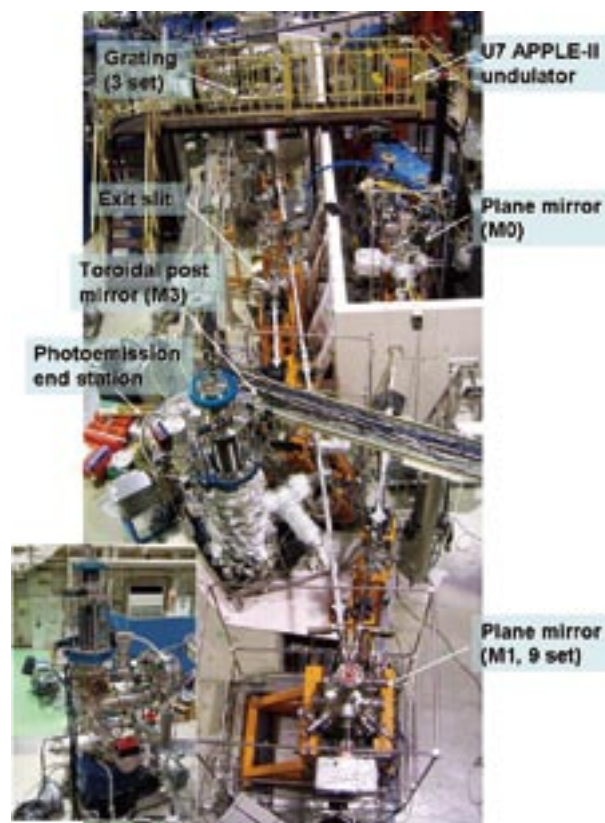


**Figure 1.** Photograph of the SAMRAI beamline consisting of the APPLE-II type undulator (U7), the modified Wadsworth type monochromator (M0–S), and the high-resolution photoemission analyzer at the focal point. The monochromator, mainly has five optical components: two plane mirrors (M0 and M1) with water cooling, one set of three spherical gratings (G), an exit slit (S), and one toroidal refocusing mirror (M3). The spherical gratings with a radius of 10 m are located 22 m from the center of the undulator. There is no entrance slit. S is located 6.47 m from G. A second branch for a VUV microscope end station is planned to be constructed after the plane mirror (M2) located between G and S.



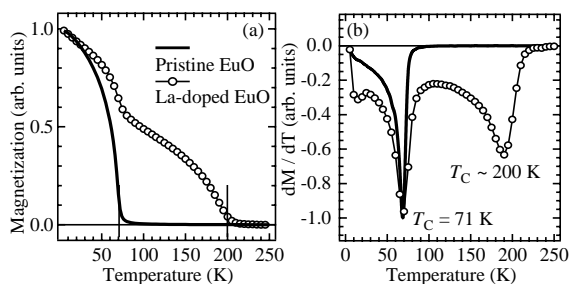


**Figure 2.** Temperature dependence of the normalized magnetization curves (a) and temperature derivative curves of the magnetization as a function of temperature (b) for fabricated La-doped EuO and pristine EuO thin films with a thickness of 100 nm on a SrTiO<sub>3</sub> substrate.

100- $\mu$ m exit slit. The beamline is used for angle-resolved photoemission spectroscopy with an energy resolution of a few meV covering the UV-to-VUV energy range.

## 2. La-Doped EuO: A Rare-Earth Ferromagnetic Semiconductor with the Highest Curie Temperature<sup>2)</sup>

We report the fabrication of single-crystalline La-doped EuO thin films with the highest Curie temperature ( $T_C$ ) of about 200 K among rare-earth compounds excluding transition metals. Due to a first-principle band calculation and an X-ray diffraction measurement, the observed increase of  $T_C$  cannot be explained only by the increase of the hybridization intensity due to the lattice shrinking and by the increase of the up-spin electrons in the Eu 5d state by the electron doping. The hybridization between the Eu 4f and donor states due to the La-substitution is a possible origin of the increases of  $T_C$ .

## 3. Design of Terahertz Pump–Photoemission Probe Spectroscopy Beamline at UVSOR-II<sup>3)</sup>

To elucidate the electronic structure relating to physical properties of solids by using selective excitations of low energy electronic and vibrational structure, a new beamline for novel pump-and-probe spectroscopy experiments combining terahertz coherent synchrotron radiation (THz-CSR) and vacuum-ultraviolet coherent harmonic generation (VUV-CHG) is designed. THz-CSR and VUV-CHG are generated from same electron bunches in the storage ring interacted with an amplitude-modulated pulse laser introduced from the outside of the storage ring. The designed schematic top view of the THz pump–PES probe beamline, BL1, is depicted in Figure 3. The amplitude-modulated Ti:Sa laser pulse (1 kHz, 10 mJ/

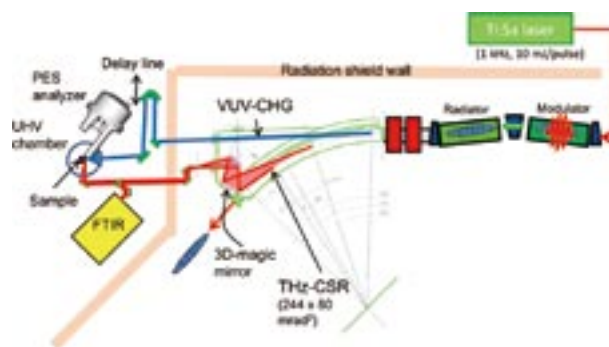


**Figure 3.** Schematic top view of the THz pump – photoemission (PES) probe spectroscopy beamline, BL1, at UVSOR-II. The light sources of PES and THz excitation are the VUV-CHG from “Radiator” and the quasi-monochromatic THz-CSR from the bending-magnet, respectively. For the THz pump – PES probe experiment, the time difference between the THz and VUV lights can be made by the delay line.

pulse) is introduced to the UVSOR-II electron storage ring. Then a periodic energy modulation is created on an electron bunch at one of two undulators, namely “Modulator,” located at the straight section. VUV-CHG is emitted from the modulated electron beam at the downstream undulator, namely “Radiator.” The modulated electron beam also produces the quasi-monochromatic THz-CSR at the bending magnet located at the downstream of the undulators. Since both THz-CSR and VUV-CHG are monochromatic lights, no monochromator for both lights is needed. However, the spectral feature of the THz-CSR must be confirmed by a Fourier transform interferometer (FTIR). Both VUV-CHG and THz-CSR are directed to the same position on a sample in an ultra-high vacuum chamber with a photoelectron analyzer located at the outside of the radiation shielding wall. The THz pump–PES probe experiment is performed as follows; At first, THz-CSR is irradiated to the sample. Just after that, VUV-CHG is irradiated to the sample and PES measured with the time delay. The time delay between the THz-CSR and VUV-CHG is made by the delay line in the optical pass of VUV-CHG. Since the expected 6-th higher harmonics ( $\sim 9$  eV) is not high photon energy, normal incident optics can be used for the delay line.

### References

- 1) S. Kimura, T. Ito, M. Sakai, E. Nakamura, N. Kondo, K. Hayashi, T. Horigome, M. Hosaka, M. Katoh, T. Goto, T. Ejima and K. Soda, *Rev. Sci. Instrum.* **81**, 053104 (2010).
- 2) H. Miyazaki, T. Ito, H. J. Im, K. Terashima, S. Yagi, M. Kato, K. Soda and S. Kimura, *Appl. Phys. Lett.* **96**, 232503 (2010).
- 3) S. Kimura, E. Nakamura, M. Hosaka, T. Takahashi and M. Katoh, *AIP Conf. Proc.* **1234**, 63 (2010).

\* from Chiba University

† Present Address; Fujifilm Corporation

‡ carrying out graduate research on Cooperative Education Program of IMS with Nagoya University

# Electronic Structure and Decay Dynamics in Atoms and Molecules Following Core Hole Creation

UVSOR Facility  
Division of Advanced Photochemistry



SHIGEMASA, Eiji                    Associate Professor  
HIKOSAKA, Yasumasa            Assistant Professor\*  
IWAYAMA, Hiroshi                Assistant Professor

The dynamics of the inner-shell photoexcitation, photoionization, and subsequent decay processes is much more complex, in comparison to outer-shell photo-processes. For instance, the inner-shell photoionization is concomitant with the excitation and ionization of valence electrons, which reveal themselves as shake-up and shake-off satellite structures in the corresponding photoelectron spectrum. The one-photon multi-electron processes, which are entirely due to the electron correlation in the system, are known to happen not only in the primary inner-shell hole creation processes, but also in their relaxation processes. Our research project is focused on elucidating the electronic structures and decay dynamics in core-excited atoms and molecules, by utilizing various spectroscopic techniques together with monochromatized synchrotron radiation in the soft x-ray region.

## 1. PCI Effects in Double Auger Decay Probed by Multi-Electron Coincidence Spectroscopy

An inner atomic vacancy created by photoionization can decay by emission of radiation or by Auger decay. For L shells, the Auger decay is generally more probable and can occur with emission of one electron (single Auger decay) or of a few electrons (multiple Auger decay). The probability of multiple Auger decay is usually lower than the probability of single Auger decay but can be high enough to allow experimental observations. Recent progress in coincidence measurements opened the path to a deeper search of the double Auger (DA) decays. DA implies that the filling of the inner-shell vacancy by an outer electron can cause the ejection of two electrons. This process is in its turn divided into the direct double Auger decay (DDA) when the two electrons are emitted simultaneously and cascade double Auger decay (CDA) when the electrons emission occurs in two steps through the creation and decay of an intermediate quasi stationary state.

PCI is known as a special kind of electron correlation associated to the interaction between the charged particles of a resonant process, through the creation and decay of an intermediate quasi stationary state. In the case of inner shell photoionization, PCI reduces to the interaction of the emitted photoelectron with the Auger electrons and with the ion field which varies during the Auger decay. PCI in single Auger decay following inner-shell photoionization is quite well documented both experimentally and theoretically, but PCI in the DA processes has been much less studied.

In the present study, we reveal and investigate the PCI effects in DA processes, using Ar 2p inner-shell ionization as an example.<sup>1)</sup> We present a systematic investigation of photoelectron spectra measured in coincidence with two Auger electrons. The PCI distortion of the photoelectron and Auger lines is shown to be important both for DDA and CDA processes. Our measurements are supported by calculations based on an eikonal approach of PCI. The results of calculations are in good agreement with the experimental data thus demonstrating the adequacy of the theoretical model to the phenomenon considered. The analysis of the experimental and theoretical results shows that the photoelectron line shape depends both on the variation of the ionic field and on the interaction with the slow Auger electron. Moreover since the line shapes for DDA and CDA processes are slightly different, their analysis allows us to extract properties of the associated DA decays.

## 2. Doppler Effect in Fragment Autoionization Following Core-to-Rydberg Excitations

The Doppler effect is known to occur when the source and observer are in motion relative to each other, leading to an apparent change in the observed frequency of the propagating wave. This effect has a wide variety of applications in many



fields, relating to the sensing of movement. In the research field of molecular physics, the sensing of nuclear motion has long been an important issue. Gel'mukhanov and co-workers predicted in 1997<sup>2)</sup> that the nuclear motion in 'ultrafast dissociation' following molecular core-level photoexcitation can be probed by the Doppler effect in emitted Auger electron. Ultrafast dissociation is a process in which the molecular dissociation at the core-excited state precedes the Auger decay and then an atomic fragment emits an Auger electron. The atomic Auger electron can possess the opposite Doppler shift depending on the direction approaching the detector or moving away from it.

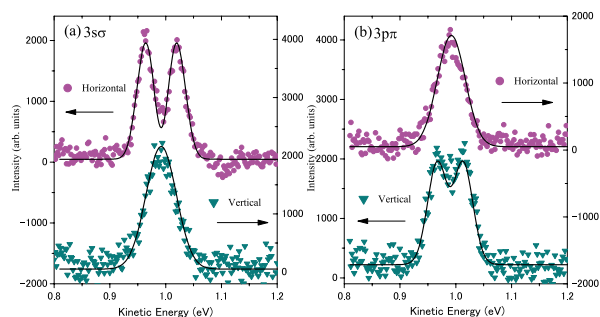


**Figure 1.** Doppler splitting observed in autoionizing electron spectra from an atomic nitrogen following the N1s to (a)  $3s\sigma$  and (b)  $3p\pi$  Rydberg excitations of  $N_2$ .

In the current work, it is demonstrated that the Doppler effect can be utilized as a new tool to study the molecular dynamics at singly-charged ion states produced by resonant Auger decay. Special attention is paid to detecting slow electrons. In cascade Auger decay, two electrons are ejected sequentially with distinct kinetic energies depending on the energy levels of the initial, intermediate, and final electronic states involved. One of the two emitted electrons is often slow (typically less than 5 eV). Singly-charged molecular ion states populated by the first electron emission can undergo competition between second electron emission and molecular dissociation. If one of the dissociating fragments is excited it may subsequently autoionize; the autoionizing atomic fragment can act as an electron emitter which can show Doppler splitting if the kinetic energy of the atomic fragment is sufficiently large and the initial photoabsorption anisotropy is substantially maintained in the angular distribution of fragments. Since anisotropic angular distributions of fragment-ions have clearly been observed in core-to-Rydberg excitations for simple linear molecules, the core-to-Rydberg excitations can be suitable precursors for observing Doppler shifts in the second step electron emissions.

As an example, the polarization dependences of the  $N^*(4d^2F^o)$  autoionization peak following the  $3s\sigma$  and  $3p\pi$  Rydberg excitations are shown in Figure 1. Clear Doppler profiles are observed in the atomic autoionization peaks, which also

display clear polarization dependences on the symmetries of the excited states. It is demonstrated that femtosecond dissociation dynamics of singly-charged ion states produced by resonant Auger decay can be deduced from the information obtained by analysis of the Doppler profiles.

### 3. Construction of a New Experimental Setup for Gas Phase Electron Spectroscopy on BL6U

Parallel to the construction program of BL6U, the installation of a new electron spectrometer for gas phase spectroscopy has been initiated. High-resolution electron spectroscopy is a powerful tool to investigate electronic structures of atoms and molecules, especially when high-resolution electron spectra and their polarization dependences are measured as a function of photon energy in high-resolution mode. The ability of this two dimensional (2D) electron spectroscopy has been demonstrated in our recent work at SPring-8,<sup>3)</sup> where a special attention is paid for detecting slow electrons following core excitations.

Figure 2 shows a photograph of the experimental setup, which is roughly composed of a vacuum chamber, a rotational mechanism, an MBS-A1 analyzer, a gas cell, and a double layer mu-metal screen. The analyzer is rotatable around the photon beam axis. The vacuum chamber and the rotational mechanism have been designed at UVSOR, and fabricated by TOYAMA Co., Ltd. The practical utilization of the new experimental setup has begun since October 2009.



**Figure 2.** A side view of the newly constructed experimental setup for gas phase electron spectroscopy on BL6U.

#### References

- 1) S. Sheinerman *et al.*, *J. Phys. B* **43**, 115001 (9 pages) (2010).
- 2) F. Gel'mukhanov, H. Ågren and P. Salek, *Phys. Rev. A* **57**, 2511–2526 (1998).
- 3) E. Shigemasa *et al.*, *New J. Phys.* **12**, 063030 (9 pages) (2010).

\* Present Address; Department of Environmental Science, Niigata University, Niigata 950-2181

# Micro Solid-State Photonics

Laser Research Center for Molecular Science  
Division of Advanced Laser Development



TAIRA, Takunori  
LOISEAU, Pascal  
ISHIZUKI, Hideki  
AKIYAMA, Jun  
TSUNEKANE, Masaki  
PAVEL, Nicolaie  
SATO, Yoichi  
MATSUSHITA, Tomonori  
JOLY, Simon  
KONG, Weipeng  
ONO, Yoko  
INAGAKI, Yayoi

Associate Professor  
Visiting Associate Professor  
Assistant Professor  
IMS Research Assistant Professor  
Post-Doctoral Fellow  
Post-Doctoral Fellow  
Post-Doctoral Fellow  
Post-Doctoral Fellow  
Post-Doctoral Fellow  
Graduate Student  
Secretary  
Secretary

The artistic optical devices should be compact, reliable, efficient and high power light sources. With the approaches of domain structures and boundaries engineering, it is possible to bring the new interaction in their coherent radiation. The high-brightness nature of Yb or Nd doped single crystal or ceramic microchip lasers can realize efficient nonlinear wavelength conversion. In addition, designed nonlinear polarization under coherent length level allows us new function, such as the quasi phase matching (QPM). The development of “*Micro Solid-State Photonics*,” which is based on the micro domain structure and boundary controlled materials, opens new horizon in the laser science.

## 1. Diode Edge-Pumped, Composite Ceramic Nd:YAG/Sm:YAG Microchip Lasers

A diode edge-pump microchip laser has a unique pumping scheme for high power operation. Low thermal distorted, high power operation is possible. The configuration of the edge-pumped microchip laser is more flexible than the well-known, thin-disk laser because there is no need to keep free space in front of the active region for pumping. Then it is possible to arrange an optical switching element such as a Cr:YAG saturable absorber or a nonlinear material close to the core, and a very short laser cavity is possible. Figure 1 shows the schematic of the diode edge-pumped Nd:YAG/Sm:YAG composite all-ceramic microchip laser (active part). The central cylindrical core with a 2mm diameter is 1.5at% Nd doped ceramic YAG. To suppress the parasitic oscillation in the microchip, the core is surrounded by 5at% Sm doped ceramic YAG as an absorber at 1064 nm which is often used as an ASE absorber. The thickness of the microchip is 0.25 mm and bonded on a Cu-W heatsink. In free running operation, the microchip laser emitted 30 mJ at an absorbed pump power of 90 mJ using the output coupler (OC) with a concave curvature of 1 m and 90% reflectivity. In passively Q-switched operation, a pulse energy of 1.76 mJ with a pulse width of 1.5 ns was obtained at an absorbed pump power of 26 mJ by inserting a Cr:YAG saturable absorber with 80% initial transmission into the cavity. The cavity length is 6 mm and the repetition rate is 10 Hz.

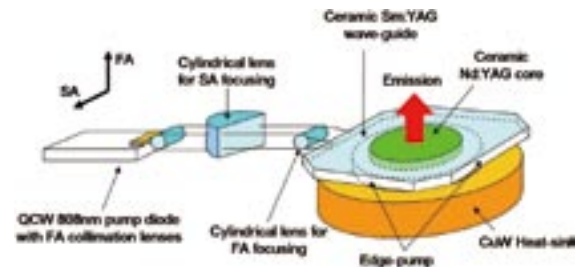


Figure 1. Diode edge-pumped Nd:YAG/Sm:YAG composite all-ceramic microchip laser.

## 2. Laser Oscillation of Nd<sup>3+</sup>-Doped Photo-Thermo-Refractive Glass under Diode Laser Pumping

The laser action of photo-thermo-refractive glass (PTR) that was the raw material of volume Bragg grating was demonstrated for the first time by introducing Nd<sup>3+</sup>. An uncoated Nd:PTR generated continuous-wave laser output of 124 mW with a slope efficiency of 25% by laser diode pumping. Nd:PTR has a wide bandwidth of 27.8 nm and 16.0 nm for emission and absorption, respectively. This enabled Nd:PTR to perform wide bandwidth laser action at 1053.9–1063.3 nm, and to hold off the decrease of pump-absorption efficiency below 30% even under 3.5-nm shift of pump wavelength from its absorption center.

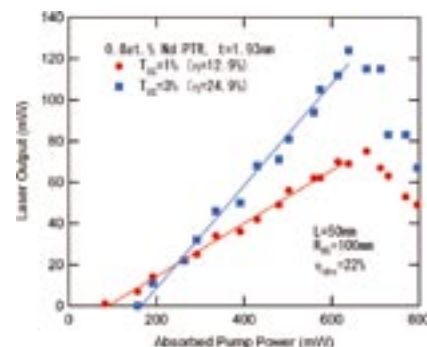
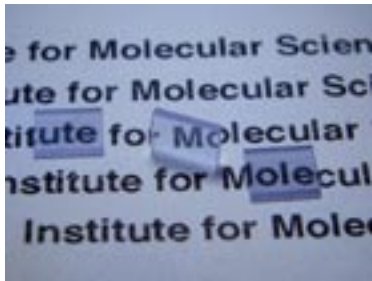


Figure 2. Laser performance of 0.8at.% Nd:PTR with output coupling of 1% and 3%.

### 3. Development of Anisotropic Transparent Ceramics for Laser Media

Trivalent-rare-earth-ion-doped ( $\text{RE}^{3+}$ -doped) transparent ceramic materials have attracted much attention as next-generation multifunctional, high-power laser gain media because they have excellent scalability and flexibility. However, fabrication of a laser-grade anisotropic (non-cubic) ceramic medium by the conventional sintering process is not possible because optical scattering occurs at randomly oriented grain boundaries. In this research, we developed a  $\text{RE}^{3+}$ -assisted magnetic orientation method and applied it for fabrication of ceramic Nd:FAP and Yb:FAP ( $\text{Ca}_{10}(\text{PO}_4)_6\text{F}_2$ , hexagonal) that have excellent optical properties such as high absorption efficiency, high emission cross-section and long emission lifetime. We successfully improved the transparency of anisotropic ceramics with loss coefficient  $<1.5 \text{ cm}^{-1}$  by optimization of material processing parameters.



**Figure 3.** Highly oriented  $\text{Nd}^{3+}$  doped fluorapatite transparent ceramics (0.5mm thickness) obtained by slip casting under 1.4T magnetic field and subsequent sintering process

### 4. High Energy Quasi-Phase Matched Optical Parametric Oscillation Using Mg-Doped Congruent $\text{LiTaO}_3$ Crystal

We report on high energy optical parametric oscillation of 118 mJ output with  $\sim 70\%$  slope efficiency in 10 ns duration of 30 Hz operation by using Mg-doped congruent composition  $\text{LiTaO}_3$  (MgLT). The periodically poled MgLT device with  $\sim 30 \mu\text{m}$  period for quasi-phase matching (QPM) in 5-mm-thick crystal are prepared. MgLT crystal could become a candidate for high-energy and higher durability material of QPM device, compared to conventional Mg-doped congruent composition  $\text{LiNbO}_3$ .

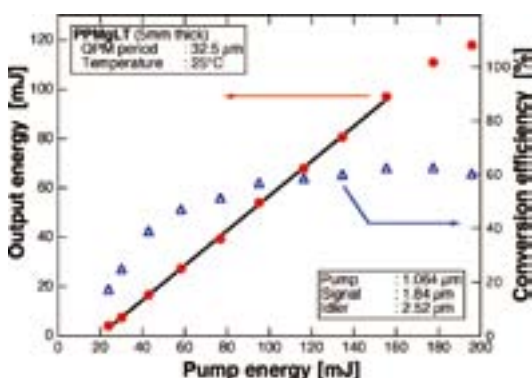


**Figure 4.** Dependence of total OPO output energy and conversion efficiency on input pump energy.

### 5. Passively Q-Switched Nd:YAG/ $\text{Cr}^{4+}$ :YAG Laser with Performances Controlled a Volume Bragg Grating

The large peak emission cross-section of Nd:YAG limits the maximum energy of a passively Q-switched Nd:YAG/ $\text{Cr}^{4+}$ :YAG laser equipped with a normal output coupler (OCM), which typically has a reduced wavelength selectivity. We demonstrated a diode end-pumped, high-peak power, passively Q-switched Nd:YAG/ $\text{Cr}^{4+}$ :YAG laser and controlled its performances with a volume Bragg grating (VBG). The laser pulse energy was increased significantly (by a factor of two or more) by elevating Nd:YAG temperature and locking the emission wavelength ( $\lambda_{\text{em}}$ ) with the VBG. Furthermore, wavelength  $\lambda_{\text{em}}$  was tuned by changing the VBG temperature, while maintaining ns-order short laser pulses of mJ-level energy.

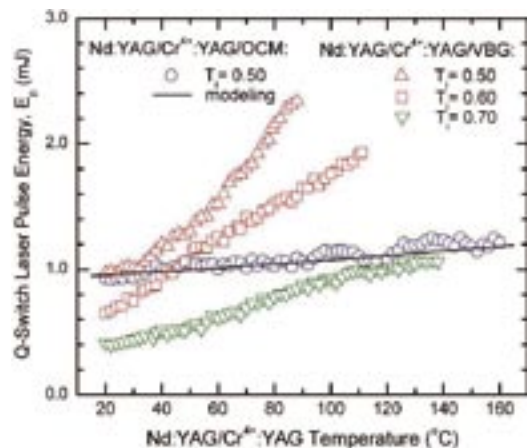


**Figure 5.** Q-switch laser pulse energy versus temperature of Nd:YAG/ $\text{Cr}^{4+}$ :YAG crystals.  $\text{Cr}^{4+}$ :YAG of various initial transmission  $T_i$ ; output coupling mirror with transmission  $T = 0.70$ ; VBG at  $20^\circ\text{C}$ .

### References

- 1) M. Tsunekane and T. Taira, *Tech. Digest of Europhoton 2010* WeP8 (2010).
- 2) Y. Sato, T. Taira, V. Smirnov, L. Glebova and L. Glebov, *Tech. Digest of Conf. on Lasers and Electro-Optics (CLEO2010)* CTuJ-4 (2010).
- 3) J. Akiyama and T. Taira, *OSA Topical Meeting on Advanced Solid-State Photonics 2010* AtuB3 (2010).
- 4) H. Ishizuki and T. Taira, *Opt. Express* **18**, 253–258 (2010).
- 5) N. Pavel, M. Tsunekane and T. Taira, *Opt. Lett.* **35**, 1617–1619 (2010).



# Ultrafast Laser Science

Laser Research Center for Molecular Science  
Division of Advanced Laser Development



FUJI, Takao  
MASUDA, Michiko

Associate Professor  
Secretary

Speed of ultrafast energy transfer from light to molecules (*i.e.* primary processes of photosynthesis, photoisomerization in visual pigments, *etc.*) is on the order of femtosecond ( $10^{-15}$  s). In our laboratory, we develop cutting edge lasers for such ultrafast molecular science, namely, femtosecond or attosecond ( $10^{-18}$  s) ultrashort pulse lasers.

For example, arbitrary waveform synthesis can be performed with simultaneous generation of femtosecond light pulses in various wavelength regions and superimposition of them with precisely controlled phases.

We would like to develop such advanced light control technology, which can push forward the research on ultrafast photochemical reactions.

I have just joined IMS since February 2010. Currently I am setting up my laboratory. In this review article, I introduce my previous works in RIKEN where I was working until the end of January 2010.

## 1. Experimental and Theoretical Investigation of a Multicolor Filament<sup>1)</sup>

Gas media, which are transparent and low dispersion in much wider range than solid media, are useful for frequency conversion of femtosecond pulses beyond the wavelength region from 0.4 to 2  $\mu\text{m}$  with keeping the pulse width short ( $<30$  fs). However, efficient frequency conversion was difficult since the nonlinearity of gas media is much smaller than that of solid media.

Recently, we have developed nonlinear frequency conversion scheme with the use of self-guiding effect of intense ultrashort pulses, namely, filamentation. By gently focusing second harmonic (400 nm,  $\omega_{\text{SHG}}$ , 0.5 mJ) and fundamental (800 nm,  $\omega_{\text{FUN}}$ , 0.5 mJ) of Ti:Sapphire laser pulses into gases, nondegenerate four-wave mixing  $\omega_{\text{SHG}} + \omega_{\text{SHG}} - \omega_{\text{FUN}} \rightarrow \omega_{\text{fwm}}$  and cascading  $\omega_{\text{fwm}} + \omega_{\text{SHG}} - \omega_{\text{FUN}} \rightarrow \omega_{\text{cas}}$  through filamentation occurred and resulted in an efficient frequency conversion to 260 nm ( $\omega_{\text{fwm}}$ , 16  $\mu\text{J}$ ) and 200 nm ( $\omega_{\text{cas}}$ , 4  $\mu\text{J}$ ). The pressure dependence of the conversion efficiency cannot be explained by a one-dimensional model, but calculation of multicolor filament by a three-dimensional model was suc-

cessful. The simulation result indicates a broad scalability of the scheme for frequency conversion of ultrashort pulses.

These two pulses were compressed by grating-based compressors sharing the same grating. The pulse widths were characterized to be 14 fs (260 nm, 4.7 eV) and 17 fs (200 nm, 6.3 eV) using a dispersion-free transient-grating frequency-resolved optical gating (TG-FROG). The results are shown in Figure 1. The energies of 260 and 200 nm pulses after the compression were 2.5  $\mu\text{J}$  and 0.5  $\mu\text{J}$ , respectively.

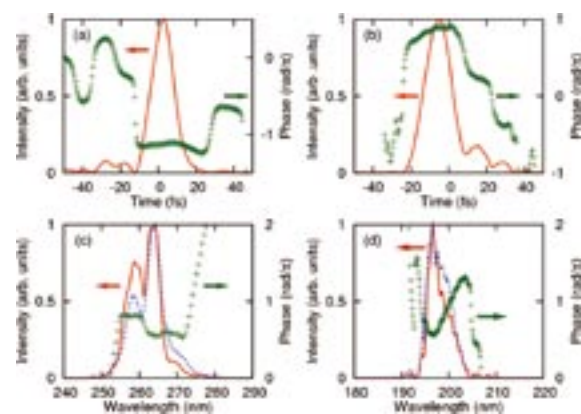


**Figure 1.** The retrieved 260 nm and 200 nm pulses obtained with TG-FROG. (a) 260 nm; time domain. (b) 200 nm; time domain. (c) 260 nm; frequency domain. (d) 200 nm; frequency domain. Solid lines show intensities and cross dots show phases. Dotted lines in the frequency-domain figures are the spectra measured by a spectrometer directly.

## 2. Time-Resolved Photoelectron Imaging of Ultrafast Internal Conversion through Conical Intersection in Pyrazine<sup>2)</sup>

The ultrashort UV pulses generated by using four-wave mixing through filamentation were used for time-resolved photoelectron imaging spectroscopy. The experimental setup is shown in Figure 2. The time resolution of the experiment was determined to be 22 fs by cross correlation of the pump and probe pulses in situ. By using the pump-probe photoelectron

imaging apparatus, a nonadiabatic electronic transition through a conical intersection in the benchmark polyatomic molecule of pyrazine was studied. The lifetimes of the  $S_2$  and  $S_3$  states of pyrazine were determined to be  $22 \pm 3$  fs and  $41 \pm 2$  fs, respectively, by the global fitting of the time-energy maps of photoelectron kinetic energy (PKE) distributions. Quantum beat with an approximately 50 fs period was observed after the  $S_2 \rightarrow S_1$  internal conversion, which was attributed to the totally symmetric vibration  $\nu_{6a}$  in  $S_1$  (see Figure 3).

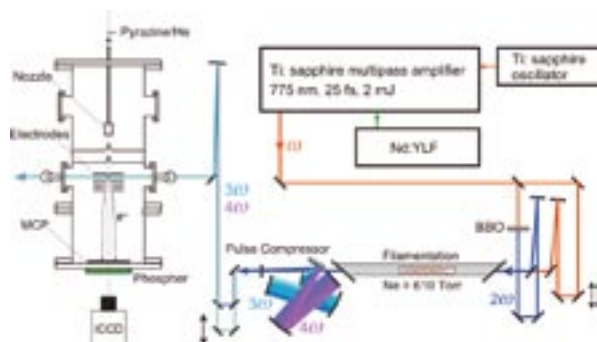


Figure 2. Schematic of the experimental setup.

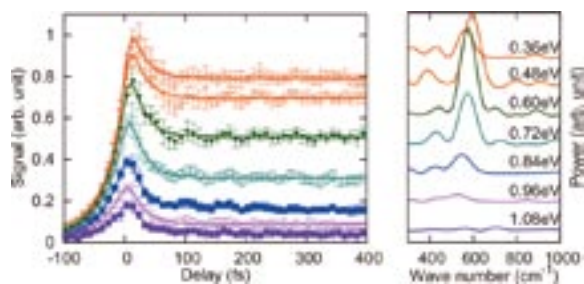


Figure 3. Time evolutions of photoelectron intensities at selected PKE subsections of pyrazine. The oscillatory features are due to the vibrational wave-packet motion along  $Q_{6a}$ . The solid lines show the results of the global fitting. Fourier power spectra of oscillatory components of photoelectron signal intensities after a delay time of 70 fs are also shown on the right panel.

### 3. Spectral Phase Transfer to Ultrashort UV Pulses through Four-Wave Mixing<sup>3)</sup>

It is very meaningful to have ultrashort VUV pulses at photoelectron spectroscopy for molecules since deactivation processes to the ground state can be explored by a probe pulse with high photon energy. Replacing the fundamental pulse in the previous scheme to output of a near infrared optical parametric amplifier, we attempted to generate pulses with shorter wavelength ( $<200$  nm). Second harmonic of Ti:Sapphire laser output (400 nm,  $\omega_{\text{SHG}}$ , 0.35 mJ) and near infrared pulses (1200 nm,  $\omega_{\text{NIR}}$ , 0.2 mJ) from a noncollinear optical parametric amplifier were gently focused into neon gas, and ultrashort pulses with the center wavelengths of 237 nm ( $\omega_{\text{fwm}}$ ) and 167 nm ( $\omega_{\text{cas}}$ ) were produced by four-wave mixing processes,  $\omega_{\text{SHG}} + \omega_{\text{SHG}} - \omega_{\text{NIR}} \rightarrow \omega_{\text{fwm}}$  and  $\omega_{\text{fwm}} + \omega_{\text{SHG}} - \omega_{\text{NIR}} \rightarrow \omega_{\text{cas}}$ , respectively. The spectra of the generated pulses are shown in Figure 4. The energy of the generated 237 nm

pulse was approximately 1.5  $\mu\text{J}$  whereas that of the 167 nm pulse were estimated to be less than 100 nJ. The reason for the lower efficiency than the previous scheme would be mode quality of NOPA output and/or phase matching condition of the nonlinear mixing. Coherence length of the phase matching ( $1/\Delta k$ ) is half of the previous four-wave mixing process.

Transfer of spectral phase from the near infrared ultrashort pulses to the UV pulses through the four-wave mixing process was also demonstrated. Assuming monochromatic second harmonic, the even order spectral phase of the near infrared pulse is transferred to the UV pulse with the opposite sign, whereas the odd order spectral phase is transferred with the same sign in principle. We controlled the spectral phase of the NIR pulses by prism insertion of a SF10 prism compressor, and measured spectral phases of the NIR pulses and the generated UV pulses by using FROG. The experimental results are shown in Figure 5. The convexities (up or down) of the spectral phase at the main part of the spectrum are opposite with each other suggesting chirp directions of the pulses are opposite with each other. Concerning the TOD, high frequency components present larger concavity compared with low frequency components in both cases. Therefore, the sign of the TOD was kept the same. A positively chirped near infrared pulse was used for generating a negatively chirped UV pulse, which was compressed down to 25 fs by a magnesium fluoride window. In principle, the spectral phase transfer scheme can also be applied to the chirp control of the generated VUV pulses.

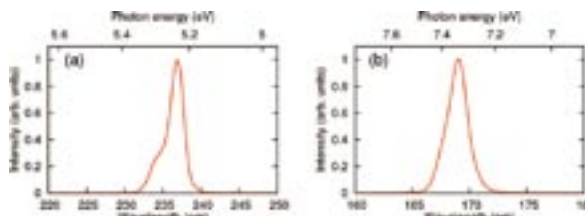


Figure 4. Typical spectra of (a) UV and (b) VUV pulses generated through the four-wave mixing and the cascaded process, respectively.

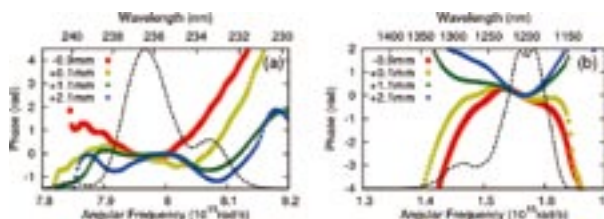


Figure 5. Spectral phases of (a) UV and (b) corresponding NIR pulses at each prism insertion. Intensity of each pulse is also shown as a dashed curve.

### References

- 1) T. Fuji, T. Suzuki, E. E. Serebryannikov and A. Zheltikov, *Phys. Rev. A* **80**, 063822 (2009).
- 2) Y.-I. Suzuki, T. Fuji, T. Horio and T. Suzuki, *J. Chem. Phys.* **132**, 174302 (2010).
- 3) P. Zuo, T. Fuji and T. Suzuki, *Opt. Express* **18**, 16183 (2010).



# Visiting Professors



Visiting Professor  
**KODAMA, Ryosuke** (from *Osaka University*)

### High Energy Density Sciences

Now it is relatively easy to realize high energy density states with high power lasers. The states would have a variety of attractive fields of sciences and technologies such as particle acceleration, laboratory astrophysics, and material science, nuclear science including medical applications and laser fusion, which is "High Energy Density Science: HEDS." One of the advantages of the HED states is its energy density, which is much higher than that of the solid state matter. He is now exploring high energy density sciences in methods of introducing a Plasma Photonics concept to control intense light and high energy charged particles with high energy density plasmas. Applying the novel geometry with plasma photonic devices, theoretical approach is being made on nonlinear optics in vacuum with super ultra-intense laser light as an extreme condition of the high energy density sciences. As his other important topics, he is interested in creation of high pressure condensed matter such as metallic solid hydrogen with high power lasers. Freezing of a higher energy density state or metallic Si have been already realized, extending the new scheme to more number of materials to have novel materials in hand, which have never seen on the earth.



Visiting Associate Professor  
**KERA, Satoshi** (from *Chiba University*)

### Electronic Structure of $\pi$ -Conjugated Organic Thin Film by Photoelectron Spectroscopy

To clarify the charge transport and injection mechanism in weakly-interacting organic molecular solids, ultraviolet photoelectron spectroscopy (UPS) is considered a conventional and novel powerful technique. Hole-vibronic coupling as well as intermolecular energy-band dispersion is important fundamental properties to reveal mysterious electric properties of organic molecular solids. Moreover, a quantitative analysis of the photoelectron angular distribution in angle-resolved UPS using photoelectron scattering theory gives us information on the molecular orbital character as well as bonding nature, leading important aspects on intermolecular and molecule-substrate interaction to electronic/spin configuration. Photoemission process related phenomena, *e.g.* scattering, interference and lifetime effect of photogenerated hole on a discrete and delocalized state of molecular orbital, are hot issue.



Visiting Associate Professor  
**UENO, Kosei** (from *Hokkaido University*)

### Nano-Imaging of Photocurrent Generation Locally Enhanced Optical Near-Fields

The development of a high-efficiency solar cell is critical in order to create a future realizing low-carbon society. To produce a solar cell with high photoelectric conversion efficiency, we need to develop a system that responds to wide spectrum of solar light, from visible to near-infrared wavelength. Nanoparticles of noble metals exhibit localized surface plasmons (LSPs) associated with enhancement of an electromagnetic field due to its localization in nanometric domains at the surface of nanoparticles. Recently, we demonstrated the plasmonic photoelectric conversion from visible to near-infrared wavelength without deteriorating photoelectric conversion by using electrodes in which gold nanorods are elaborately arrayed on the surface of TiO<sub>2</sub> single crystal. IQE measurements allowed us to elucidate the photo induced electron transfer from gold nanorods to TiO<sub>2</sub> resulting from the excitation of the LSPs is nonlinearly induced not only by optical antenna effects but also by electromagnetic field enhancement effects. To study the effect in detail, it is important to pursue where the photocurrent generation is locally enhanced at the gold nanoblocks. We are trying to measure a high-resolution image of the photocurrent generation using near field light as a local excitation source, which is obtained from an optical probe working on a near-field optical microscope.



Visiting Associate Professor  
**TAKAHASHI, Toshiharu** (from *Kyoto University*)

### Development of New Spectroscopic Methods Using THz Coherent Synchrotron Radiation

We are developing new spectroscopic techniques using a brilliant light source in the THz-wave region, *i.e.*, coherent synchrotron radiation (CSR) from short bunches of relativistic electrons. One is the technique of the scanning near-field transmission and reflection microscopy in the THz-wave region, where the high special resolution below the diffraction limit is available. On the other hand, the method of the THz pump-photoemission probe spectroscopy (PES) is also developing. Since the VUV radiation by the coherent harmonic generation (CHG) can be emitted using the laser pulse in UVSOR, the jitter-free pump-probe spectroscopy is possible with the THz-CSR. In order to perform these spectroscopic techniques, we are constructing a new CSR beamline in UVSOR.